DOI:10.14753/SE.2023.2809

THE ROLE OF PHYSICAL AND PHARMACOLOGICAL PREHABILITATION IN ACCELERATED LIVER REGENERATION

PhD thesis

Noémi Daradics MD

Károly Rácz Doctoral School of Clinical Medicine

Semmelweis University

Supervisor: Attila Szijártó MD DSc

Official reviewers:

Nóra Sydó MD PhD

Norbert Németh MD DSc

Head of the Complex Examination Committee:

Péter Sótonyi MD DSc

Members of the Complex Examination Committee:

Andrea Ferencz MD PhD

Kristóf Dede MD PhD

Budapest, 2023

DOI:10.14753/SE.2023.2809

Table of Contents

DOI:10.14753/SE.2023.2809

DOI:10.14753/SE.2023.2809

DOI:10.14753/SE.2023.2809

List of Abbreviations

3D SPECT: 3-dimensional single photon emission computed tomography

ALPPS: associating liver partition and portal vein ligation for staged hepatectomy

ALT: alanine-aminotransferase

AST: aspartate-aminotransferase

ATP: adenosine-5'-triphosphate

BA: bile acid

BSEP: Bile Salt Export Pump

CT: computed tomography

CTP score: Child-Turcotte-Pugh score

Cyp7a1: cytochrome P450 isoform 7A1

CypD: Cyclophilin D

FGF: fibroblast growth factor

FLR: future liver remnant

FLRV: future liver remnant volume

Fox: Forkhead box

FXR: farnesoid X receptor

HBS: hepatobiliary scintigraphy

ICG: indocyanine green

INR: international normalized ratio (INR)

KO: knockout

mPTP: mitochondrial permeability transition pore

MRI: magnetic resonance imaging

MRP: multidrug resistance-associated protein

NAD(P)H: nicotinamide adenine dinucleotide phosphate

NRF: nuclear respiratory factor

Ntcp: sodium/taurocholate cotransporting polypeptide

OATP: organic-anion-transporting polypeptide

PGC: peroxisome proliferator-activated receptor-gamma coactivator

PHLF: post hepatectomy liver failure

PP: physical prehabilitation

Ppif: Peptidyl-prolyl cis-trans isomerase F gene

PVE: portal vein embolization

PVL: portal vein ligation

PVO: portal vein occlusion

RGS: rat grimace scale

S: sedentary

tBil: total bilirubin

TLV: total liver volume

WT: wild type

DOI:10.14753/SE.2023.2809

1. Introduction

Over the past decades the limitations of liver surgery have been overcome. By improving intensive care and anesthetic methods, deepening our knowledge of hepatic anatomy and refining surgical technique, new doors have opened in the operating room and the boundaries of accomplishing safe liver resections are continually widening (1). Currently, in this era of liver surgery, the main and most important restraint of curative resection is the insufficient volume and function of future liver remnant (FLR) following operation (2). To overcome this restrictive factor and further broaden the indication of major liver resections, augmentation techniques have been invented to push patients from unresectable to resectable status by inducing liver regeneration. Portal vein occlusion (PVO) techniques are standardly used in hepato-pancreato-biliary surgery to preoperatively increase FLR size, however more than a third of patients must be excluded from performing major hepatectomy due to the insufficient growth rate of the FLR after PVO, which requires time. Unfortunately, concurrent tumor progression could compromise the second stage of the procedure (3,4). To overcome these major issues a novel surgical procedure, associating liver partition and portal vein ligation for staged hepatectomy (ALPPS), was introduced, which could induce a more rapid and robust regeneration, offering a therapeutic approach for patients initially considered unresectable (5). High postoperative morbidity and mortality were reported initially following ALPPS (6). In order to access the full potential of ALPPS novel approaches must be found to mitigate the adverse postoperative outcome. Prehabilitation is a new multimodal concept in oncological surgery, aiming to increase a patient's bearing capacity while decreasing perioperative stress (7). Although promising results have been described concerning liver surgery, no literature data regarding the effect of prehabilitation on the outcome of two-stage hepatectomies as PVO and ALPPS is available.

DOI:10.14753/SE.2023.2809

1.1. Limitations of the surgery in the treatment of liver malignancies

1.1.1. The relevance of post-hepatectomy liver failure and the future liver remnant

Primary and metastatic liver malignancies are one of the leading causes of cancer-related deaths, putting a huge burden on health care systems worldwide (8,9). Although oncological treatment rapidly evolved over the last few decades, the only curative treatment option of hepatic tumors is the surgical removal of the malignant tissue. Unfortunately, due to the often late discovery of liver malignancies and consequently the large tumor load by the time of the diagnosis, approximately 45% of patients necessitate extended liver resection for curative treatment (10). Despite the immense regeneration capacity and functional reserve of the liver, excessive surgical eradication of large hepatic tumors aiming R0 (microscopically tumor-free-margin) resection could lead to post hepatectomy liver failure (PHLF) (11,12). Although the development of surgical and critical care contributed to the decrease of mortality below 5% after hepatectomies, a significant proportion (up to 35%) is still related to PHLF (13). Depending on the severity of PHLF, the postoperative mortality varies between 40% and 60%, amounting to the most important cause of death after major and extended hepatectomy (14–16).

In 2011 the International Study Group of Liver Surgery has defined PHLF as *"a postoperatively acquired deterioration in the ability of liver to maintain its synthetic, excretory and detoxifying functions, which are characterized by an increased INR and concomitant hyperbilirubinemia on or after postoperative day 5"* (17). Various factors play role in the onset of PHLF, such as the general condition of the patient (age, obesity, diabetes), the liver parenchyma (cholestatic, cirrhotic, steatosis, chemotherapy) and other, surgical intervention related risk factors (loss of blood, infection, sepsis, liver ischemia, portal hypertension) (17). However, the most important cause of PHLF is the insufficient volume and function of the FLR after hepatectomy (12). Therefore, the accurate preoperative measurement of the FLR has become a crucial point to perform safe and successful liver resections. Minimum FLR volumes have been generally accepted . FLR > 20-25%, for patients with healthy liver parenchyma, FLR >30% for those who have

received chemotherapy for longer than 12 weeks and FLR > 40–50% and in case of fibrosis or cirrhosis an (18).

1.1.2. Preoperative volumetric assessment of the future liver remnant

The importance of volumetric assessment lies in the fact that the segmental distribution of the liver is not uniform and varies from patient to patient, hence the sufficient FLR cannot be estimated based on the traditional anatomic nomenclature (19). Therefore, to safely perform major hepatectomy, preoperative hepatic volumetric analysis is inevitable.

Generally, standardized FLR is expressed as a percentage of total liver volume (TLV) without tumor volume, which could be measured by medical imaging or estimated using the following formula validated by meta-analysis on western population: TLV (cm^3) = -794.41 + 1267.28 × body surface area (m^2) (20,21). 3-dimensional computed tomography (CT) and magnetic resonance imaging (MRI) volumetry has been shown to accurately assess FLR and TLV volume (22), although measurement of the latter using medical imaging might be troublesome in case of large tumors, biliary disease, or underlying liver disease, as these pathological processes could alter TLV (18).

1.1.3. Preoperative functional assessment of the future liver remnant

Although volumetric FLR analysis still serves as the standard measurement to reduce the risk of PHLF (23,24), preoperative evaluation of liver function is of utmost importance in the determination of resectability, as mortality and morbidity rates displayed strong correlation with the degree of hepatocellular dysfunction (25,26). However, the comprehensive functional hepatic assessment encounters various difficulties due to the multiple and diverse functions of the liver (18). While numerous grouping systems exist, the most plausible is the classification based on the dynamic of the function tests. More specifically, we can distinguish *static liver function tests and scoring systems* and *dynamic liver function tests*. The currently available liver function tests are summarized in Table 1. Due to the length limitations, only the most important test modalities were exerted in detail.

DOI:10.14753/SE.2023.2809

Table 1. Liver function tests. Based on Bennink RJ. et al: Semin Nucl Med, 2012

Static liver function tests	
Assessed parameter	**Relevance**
prothrombin, INR	synthetic function
albumin	synthetic function
bilirubin	uptake, conjugation, excretion
alkaline phosphatase	cholestasis, biliary obstruction
gamma-glutamyl transferase	cholestasis, alcohol abuse
alanine aminotransferase	liver damage, necrosis
aspartate aminotransferase	liver damage, necrosis

Score systems	
Score system	**Assessed parameter**
Child-Turcotte-Pugh	albumin, bilirubin, prothrombin, ascites, encephalopathy
MELD (model for end-stage liver disease)	bilirubin, creatinine, INR, etiology

Dynamic liver function tests	
Assessment	**Relevance**
Antipyrine clearance test	microsomal function
Lidocaine clearance test (MEGX)	microsomal function
Galactose tolerance test	cytosolic function
Indocyanine green (ICG) clearance test	liver perfusion, anion excretion
^{99m}Tc-galactosyl (GSA) scintigraphy	liver perfusion, anion excretion
^{99m}Tc-mebrofenin scintigraphy	liver perfusion and function

Static liver function tests and scoring systems

Initial evaluation of liver function includes the measurement of albumin, prothrombin and international normalized ratio (INR) to assess the biosynthetic function of the liver, pseudocholinesterase, which characterizes the parenchymal reserve and bilirubin reflecting on the elimination capacity (27). In addition, liver transaminases (aspartate- and alanine-aminotransferase (ALT, AST)) are also frequently measured. Although these do not describe liver function, they are useful indicators of liver necrosis (27).
Two commonly used scoring systems have been developed based on these parameters to evaluate liver function. The model for end-stage liver disease (MELD) takes into account patients' bilirubin, INR and creatinine (28). While it was developed to predict survival in cirrhotic patients following transplantation, the MELD score is currently utilized in a wider spectrum of liver diseases, including the preoperative assessment hepatectomy (29). Various modifications of the MELD score have been introduced enabling more precise evaluation (14). On the contrary, the Child-Turcotte-Pugh (CTP) score is based on both clinical measures - including ascites and encephalopathy – and laboratory indicators of liver function as total serum bilirubin, INR and serum albumin (30). CTP score is also frequently used in the preoperative evaluation of hepatectomy, as its elevated value is associated with higher morbidity and mortality rates (31).

It is important to bear in mind that static liver function tests and scoring systems are not fully effective methods to evaluate liver function due to multiple reasons. First, according to the nomenclature, they only show a momentary insight into hepatic function. Second, they are not specific and sensitive enough to reliably predict function. Third, as a serum parameter they only reflect on the whole liver function and are not able to distinguish between the different parts of the liver (27,32).

DOI:10.14753/SE.2023.2809

Dynamic liver function tests

Instead of only showing cross-sectional data of hepatic function, dynamic liver function tests reflect on the liver function during a longer time period, while particular types could show both regional and global liver function, facilitating a more precise and relevant evaluation of hepatic function. Indocyanine green (ICG) clearance is the most frequently used assessment tool for the preoperative evaluation of hepatic function before major hepatectomy. ICG is a water soluble inert tricarbocyanine, which is selectively absorbed by hepatocytes and excreted in bile (33). Most commonly the test displays the percent of serum clearance of ICG after 15 minutes, which indicates both the blood flow of the liver and the hepatocyte functional capacity, however the results reflect only the function of the whole liver (2). In contrast, scintigraphy based on nuclear medicine could selectively show regional hepatic function along with the whole liver function, completely redefining the preoperative assessment possibilities of the FLR (27). While ^{99m}Tc-galactosyl serum albumin test is not typically used outside Japan (27,34), ^{99m}Tc-mebrofenin hepatobiliary scintigraphy (HBS) is a commonly available test to evaluate FLR function (Figure 1). Mebrofenin is specifically taken up by organic-anion-transporting polypeptide (OATP)1B1 and -B3 in hepatocytes and excreted in the bile by multidrug resistance-associated protein (MRP)2 without biotransformation and enterohepatic circulation (35,36). As the detection of ^{99m}Tc-mebrofenin with 3-dimensional single photon emission computed tomography (3D SPECT) could accurately detect both the FLR volume (FLRV) and its function (27), it has earned high clinical relevance in liver surgery and is utilized with growing frequency (36–38).

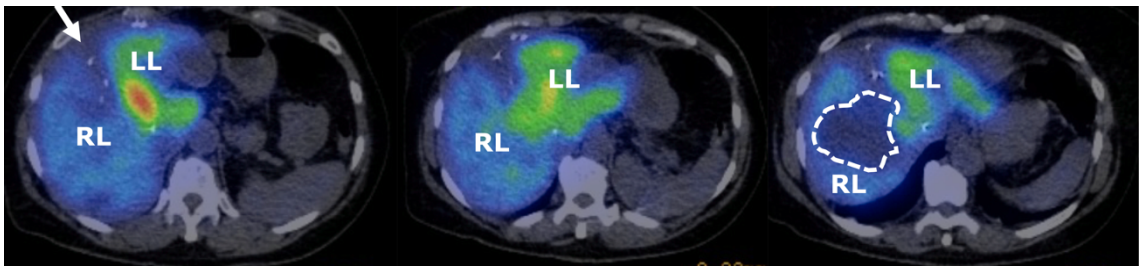

Figure 1. ^{99}mTc-mebrofenin single photon emission computed tomography (SPECT) hepatobiliary scintigraphy on the 10th postoperative day after ALPPS. Inhomogeneity could be observed in the distribution of the tracer between the tumor containing (dashed line) right lobe (RL) and left lobe (LL) of the liver. As the RL was ligated and the liver was transected (arrow)

between the RL and LL, the tracer intensity in the RL decreased, while in the LL, which is the FLR, increased. The figure was created by the author from the database of the Department of Surgery, Transplantation and Interventional Gastroenterology, Semmelweis University.

1.2. Increasing resectability with liver volume manipulation techniques

1.2.1. Portal vein occlusion

PVO techniques were developed to promote FLR hypertrophy in order to expand the safety zone of major hepatectomy without increasing morbidity or mortality (39–41). The essence of this method is the occlusion of the portal vein leading to the tumor bearing lobe with embolization (portal vein embolization, PVE) or ligation (portal vein ligation, PVL), inducing ipsilateral atrophy and contralateral hypertrophy of the liver (42). The exact mechanism underlying the induced regeneration has still not been fully understood, however it has been stated that peri-portal inflammation along with the alteration of portal venous blood flow plays a key role in generating hypertrophy stimuli (43). Today, the PVE technique is standardly implemented as an alternative first step of two-stage hepatectomy when the FLR is considered to be insufficient in size and/or function and hence the induction of FLR hypertrophy is desired (1). After reaching sufficient FLR hypertrophy, resection of the tumor bearing lobes could be performed during the second step of the two-stage hepatectomy (42). Unfortunately, the PVO method also encounters drawbacks. The augmentation of the FLR requires 4-8 weeks, whilst tumor progression could occur compromising the second step of the two-stage hepatectomy. Additionally, the FLR growth rate is not always adequate to meet the criteria of performing safe resection. These major issues of the traditional two-stage approaches could result in a drop-out of patients up to 35% (4).

1.2.2. Associating liver partition and portal vein ligation for staged hepatectomy

Increasing the rate of the FLR regeneration is crucial. ALPPS is a novel modification of two-stage hepatectomy enabling safe resection of patients considered inoperable by standard approaches (Figure 2) (6). Initially introduced as the combination of PVL and “in situ split” in 2007 (44), ALPPS induces a more effective stimulation of the residual

liver growth, resulting in not only more robust FLR expansion, but also within a shorter time period of 6 – 10 days (45). Despite the initial worldwide enthusiasm, skepticism raised regarding ALPPS, as the reported mortality and morbidity rates after the surgery triggered an intense debate about the safety of the procedure (46–48). Therefore, in 2015 a consensus meeting was organized in Hamburg, where strict selection criteria were created considering not only the disease of the patient, but also the performance status and technical aspects (49). Although the new recommendations have led to the improvement of postoperative outcome, the patomechanism behind the unfortunate mortality and morbidity rates are still not fully elucidated. It has been previously stated by various studies that despite the seemingly adequate FLR volume, the functional recovery of the regenerating liver is delayed, resulting in a reciprocity between volume and function (32,37,50). In our previous study we identified that impaired mitochondrial function and biogenesis could be accounted for the lagging functional regeneration after ALPPS (51). In light of the exceptional benefits of ALPPS, investigating further the pathomechanism of volumetric and functional regeneration, as well as identifying molecular targets to establish novel therapeutic approaches, would undoubtedly contribute to the improved survival of liver cancer patients.

DOI:10.14753/SE.2023.2809

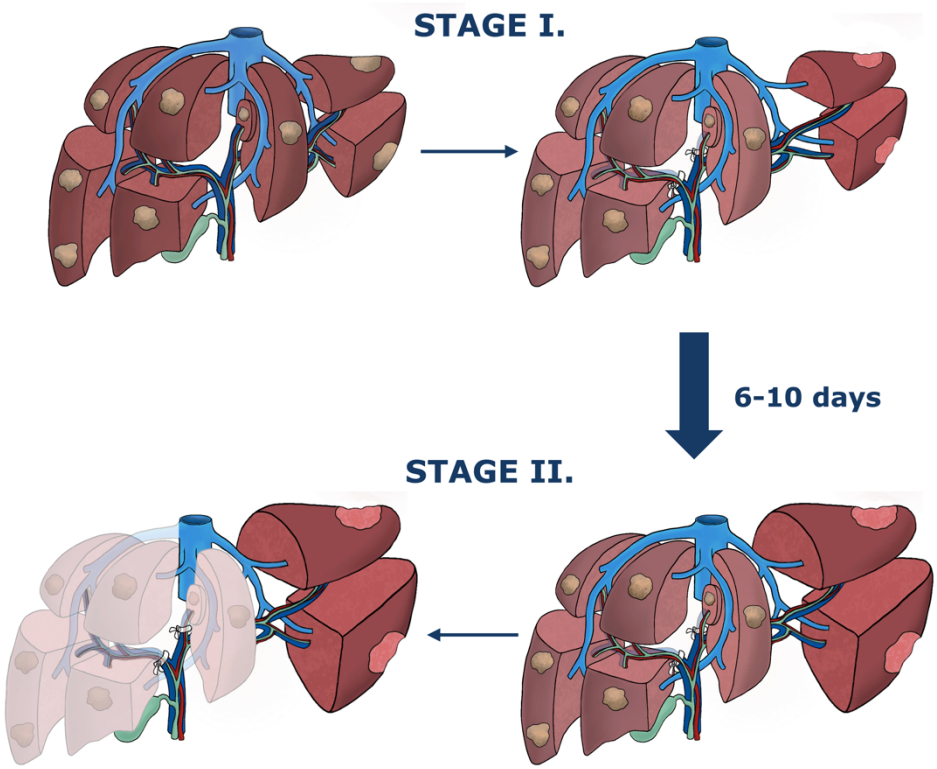

Figure 2. ALPPS procedure. During stage I. the ligation of portal veins leading to the tumor bearing lobes is performed and liver parenchyma is transected along the intended line of resection and the future liver remnant (FLR) cleaned by partial resections from all tumor tissue in the case of bilobar tumors. The patient is then allowed to recover, whilst the FLR growth occurs. After a waiting period of 6-10 days stage II. is performed in which the deportalized liver is removed to render the patient completely tumor-free. The figure was created by the author.

DOI:10.14753/SE.2023.2809

1.3. Prehabilitation

A novel concept arised in the last few years in oncological surgery, called prehabilitation. This multimodal approach is defined as *"a process in the continuum of care that occurs between the time of diagnosis and the beginning of treatment and includes physical, nutritional and psychological assessments that establish a baseline functional level, identify impairments, and provide interventions that promote physical and psychological health to reduce the incidence and/or severity of future impairments"* (7).

Results in oncological surgery suggest that prehabilitation has a positive impact on postoperative recovery, and could potentially improve outcomes in oncological care (7). Most data reported originate from colorectal and general surgical field, showing improvement in physical function and in the length of hospital stay, however, these beneficial effects have not yet been translated into improvements of mortality and morbidity (52–56). This could be due to the increased rate of vulnerable patients, who could not tolerate the extra physical burden and/or the inadequately chosen prehabilitation modalities.

In addition, data are scarcer and more controversial regarding the effects of prehabilitation in liver surgery (57–60), with no published data on two-stage hepatectomies (PVO or ALPPS). Properly implemented investigations would be specifically important for this subset of patients due to multiple reasons. First, major liver resection, particularly ALPPS is a procedure with significant mortality and morbidity. Second, patients undergoing liver surgery have already compromised status due to chronic liver disease, and the associated sarcopenia, malnutrition, coagulopathy, and other multiorgan effects (61). Physical frailty has been reported by various study a predictor of clinical outcomes in patients with cirrhosis and advanced or end-stage liver disease (62), therefore investigating prehabilitation could contribute to the successful surgical treatment of liver cancer patients, decrease the postoperative mortality and morbidity and improve the outcome of the oncological treatment.

Aiming to set up reproducible models, we have analyzed separately different modalities within prehabilitation, thereby reducing the errors originating from the usage of inordinate variables.

1.3.1. Physical prehabilitation

One crucial pillar of prehabilitation is physical prehabilitation (PP), which improves the functional status of the patient by various types of exercises. Physical fitness is considered a modifiable and treatable factor during the preoperative phase even in old and frail patients (63) and even in a short timeframe before surgery (64).

Evidence demonstrate that preoperative exercise reduces morbidity and the length of hospital stay in cardiac surgery (64) and improves functional recovery after thoracic surgery (65). In abdominal surgery physical activity and fitness are strongly associated with the postoperative outcomes such as mortality, length of stay and functional recovery (66). Nevertheless sufficient evidence is not yet available for the prevention of postoperative complications, as most studies investigating the subject lack statistical power.

Despite the well-established effects of exercise on improving the systemic tolerance to perturbation, the mechanisms by which particular organs are protected from surgical stress and injury remained ambiguous. It has been already shown that exercise initiates metabolic reprogramming and creates an anti-inflammatory environment in many cell types, including hepatocytes (67–69). Preoperative exercise also significantly attenuates liver injury and inflammation from ischemia and reperfusion in the liver (70). In our previous study we also demonstrated that PP improves the damaged mitochondrial function and enhances the level of the master-regulator of mitochondrial biogenesis peroxisome proliferator-activated receptor-gamma coactivator (PGC)1-α and its target protein nuclear respiratory factor (NRF)1 following ALPPS (71). However, well-designed, mechanistic studies on the effect of preoperative exercise therapy are still lacking regarding major liver surgery, while there is no data to our knowledge regarding the effect of PP on ALPPS, which are hampering the comprehensive application of such a highly useful, easily utilizable, non-pharmacological therapeutic strategy.

1.3.2. Pharmacological prehabilitation

The assessment of the signaling pathways regulating accelerated liver regeneration after ALPPS could help to identify pharmacological targets. By pharmacologically influencing these target molecules, beneficial effects similar to the ones of PP could be achieved in case of frail, weakened patients, who could not tolerate extra physical burden.

Mitochondrial therapy

According to our previous studies (51,71), the improvement of mitochondrial dysfunction could contribute to better postoperative outcomes following ALPPS. The inhibition of Cyclophilin D (CypD) has recently emerged as an effective mitochondrial therapy in hepatic diseases (72). CypD, encoded by the *Peptidyl-prolyl cis-trans isomerase F* gene (*Ppif*), is a protein in the matrix of the mitochondria (73). Functioning as a master regulator of the mitochondrial permeability transition pore (mPTP), which is a calcium efflux channel, CypD could induce the deregulated release of calcium and pro-apoptotic factors (i.e. cytochrome c) from the inner mitochondrial space (72–74). These mechanisms trigger the activation of caspases generating apoptotic cell death (72,75).
Apoptosis is fundamental in liver regeneration induced by two-stage hepatectomies (43), therefore the regulation of mPTP opening could have a considerable effect via altered apoptosis on the accelerated liver regeneration. The non-regulated opening of mPTP also ensues the nonspecific transport of aqueous solutes up to a molecular weight of 1,5 Da causing the depolarization of mitochondria and the failure of the oxidative phosphorylation (73) (Figure 3).
Although there is no literature data regarding the effect of CypD inhibition after two-stage hepatectomy as PVL or ALPPS, previous studies showed that pharmacological inhibition of the CypD reduces hepatic injury (76,77), and ischemic liver damage (78). It has been also evidenced that CypD inhibition has beneficial effect on hepatocyte injury after hepatitis-C infection (79), and quarter-size liver transplantation (80) promoting that CypD inhibition could be an effective therapeutic strategy to mitigate the adverse postoperative outcome of ALPPS.

DOI:10.14753/SE.2023.2809

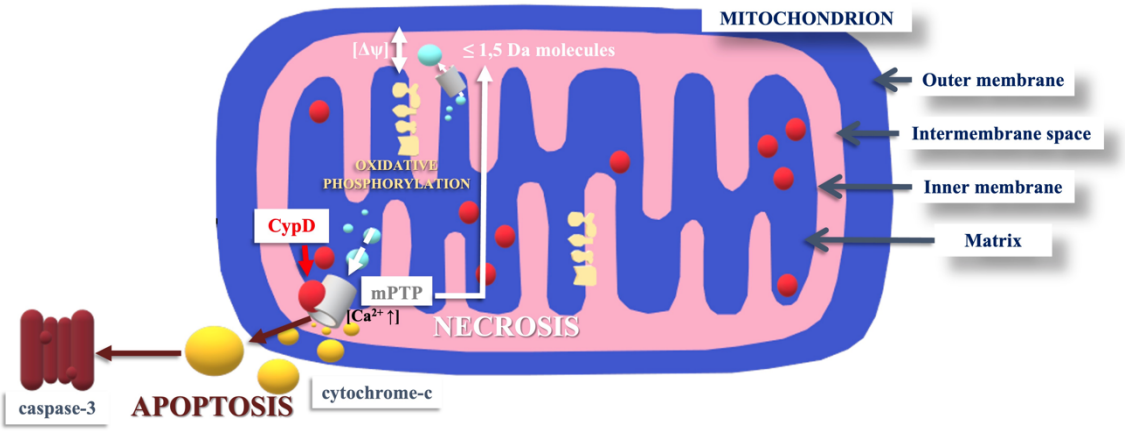

Figure 3. The effects of Cyclophilin D (CypD) on mitochondrial function. CypD via the opening of mitochondrial permeability transition pore (mPTP) induces the deregulation of calcium (Ca^{2+}) release and pro-apoptotic factors (i.e. cytochrome-c) from the inner mitochondrial space, triggering the activation of caspases (i.e. caspase-3) and generating apoptotic cell death. The non-regulated opening of mPTP also ensues the nonspecific transport of aqueous solutes up to a molecular weight of 1,5 Da causing the depolarization of mitochondria and the failure of the oxidative phosphorylation. The figure was created by the author.

Utilization of the bile acid induced signaling pathways

Bile acids (BA) play a key role in the early phase of liver regeneration (81). BAs with mitotic properties act as signaling molecules by activating the nuclear BA receptor farnesoid X receptor (FXR), which triggers hepatocyte proliferation (82) (2. Figure). Therefore, it is plausible that liver regeneration signals following ALLPS are also regulated by BAs.

Hepatectomy results in the rise of BA level in the remaining hepatocytes, which could in turn induce regeneration signals (83–85). Therefore, when bile flow is disrupted, liver regeneration is stalled, possibly due to hampered FXR signaling. Supporting that FXR signaling is essential for normal liver regeneration, liver regrowth is significantly impaired in *Fxr*-deficient mice (82,86).

As FXR is expressed both in hepatocytes and enterocytes, it steers consequently a hepatic and intestinal route of liver regeneration (Figure 4) (87). Considering that the deletion of hepatic *Fxr* delays liver regeneration (86), it might be conceivable that the primary

activator of liver regeneration is the intestinal FXR signaling. After initiating from enterocytes, the intestinal FXR pathway induces the production of mitogenic fibroblast growth factor (FGF)19 (FGF15 orthologue in rodents), which regulates BA synthesis and activates liver regeneration via the hepatocyte FGFR4 receptor (88). Study investigating FGF15-deficient mice evidenced the crucial role of FGF15 in the hepatic regenerative process, as significant impairment of liver regrowth was observed (89). Although the role of FXR pathway in liver regeneration following PVL has already been described (90–92), the relevance of the hepatic and intestinal pathways has not yet been distinguished. Also, at the time of the study, there was no literature data regarding FXR signaling after ALPPS.

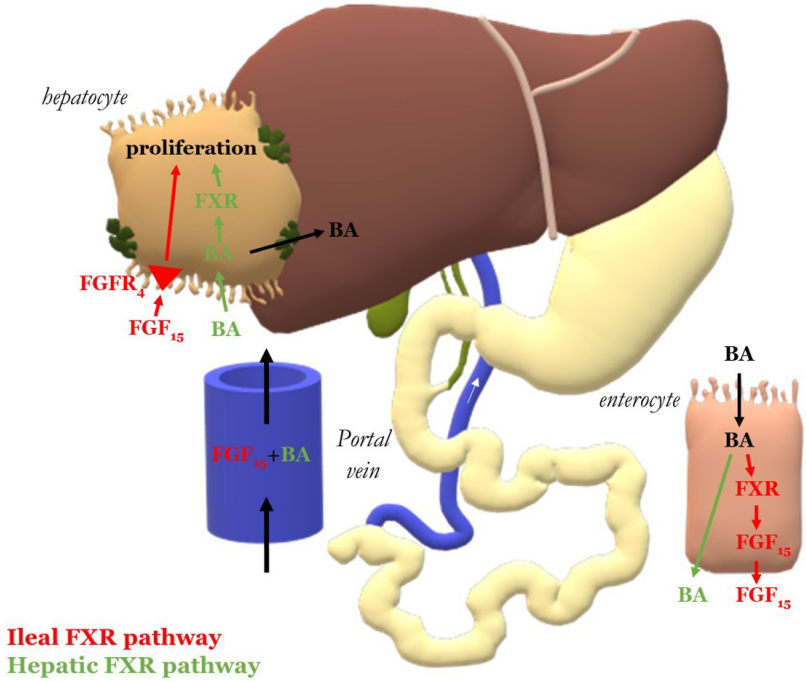

Figure 4. Bile acid (BA) and farnesoid X receptor (Fxr) signaling. Ileal Fxr pathway (red marking): The absorbed BAs activate FXR signaling in the ileal enterocytes, inducing the production of mitogenic fibroblast growth factor (FGF)15. After entering the portal circulation, FGF15 binds to hepatocytes and activates the regeneration pathway via the FGFR4 receptor. Hepatic FXR pathway (green marking): absorbed BAs enter the portal circulation and reach the hepatocytes, where they activate hepatocyte FXR signaling and initiate proliferation. Figure was adapted without modifications from: Daradics N. et al: Curr Oncol 2021.

DOI:10.14753/SE.2023.2809

2. Objectives

In our translational studies we aimed to identify potential preoperative therapeutic approaches to mitigate the adverse postoperative outcomes of ALPPS by investigating the effects of "physical prehabilitation" and identifying molecular targets to create the ground of the "pharmacological prehabilitation".

Aims of the I. experiment

In the I. experiment we aimed to investigate the effect of physical prehabilitation on the postoperative outcome of ALPPS in a rodent model by demonstrating:

I./1 the effect of physical prehabilitation on postoperative volumetric liver regeneration,
I./2 the effect of physical prehabilitation on postoperative functional liver regeneration,
I./3 the effect of physical prehabilitation on postoperative vulnerability in endotoxemia model,
I./4 the effect of physical prehabilitation on body composition,
I./5 the connection between changed body composition and improved postoperative outcome.

Aims of the II. experiment

In the II. experiment we aimed to investigate the effect of CypD depletion on mitochondrial function, biogenesis and liver regeneration after ALPPS in a mice knockout (KO) model by demonstrating:

II./1 the effect of CypD depletion on mitochondrial function,
II./2 the effect of CypD depletion on mitochondrial biogenesis,
II./3 the effect of CypD depletion on liver regeneration.

DOI:10.14753/SE.2023.2809

Aims of the III. experiment

In the III. experiment we aimed to investigate the function of bile acids in liver regeneration and the involvement of hepatic and intestinal FXR signaling after ALPPS juxtaposed to PVL in rodent model by demonstrating:

III./1 the liver regeneration after ALPPS in comparison to PVL,
III./2 the hemodynamical changes after ALPPS in comparison to PVL,
III./3 the systemic and portal bile acid concentration after ALPPS in comparison to PVL,
III./4 the expression of bile acid transporters and production enzymes after ALPPS in comparison to PVL,
III./5 the hepatic and ileal FXR signaling pathway after ALPPS in comparison to PVL.

3. Methods

All experiments were performed in accordance with the relevant guideline of the directive 2010/63/EU of the European Parliament, and all methods were reported in accordance with the ARRIVE guidelines (93). Experiments were approved by the Scientific Ethical Committee on Animal Experimentation of the National Department of Food Chain Safety (approval number: PEI/001/1732-6/2015, PEI/001/1732-6/2015, PE/EA/1843-6/2016). Animals were housed in 12-hour day-night cycle, with temperature (20-22 °C) and humidity (40-70%) controlled environment. Ad libitum access to water and standard chow (Toxicoop, Hungary) was provided. Before the inclusion to the experiment, animals were acclimated for 7 days.

Liver weight measurement and the analysis of cell proliferation in each experiment:
"Each liver lobe was measured separately using an analytical scale (model AG245, Mettler Toledo, Columbus, OH, USA). Percentual increase in liver mass was calculated using the following formula: (lobe weight / body weight at the time of death) / (mean lobe weight at preoperative time point/ body weight at preoperative time point) × 100%.
From the formalin fixed paraffin embedded (FFPE) liver tissue specimens, 4-µm thick sections were cut, deparaffinized in xylene (2 × 10 min), and rehydrated in graded alcohol series. Antigen retrieval was performed at pH = 6.0 (S2031, Agilent, Santa Clara, CA). Ki67 immunohistochemistry was performed using anti-Ki67 antibodies (ab16667, Abcam, Cambridge, UK) according to the manufacturer's instructions. Counterstaining was performed with hematoxylin. The histological slides were scanned with a Pannoramic P1000 slide scanner system (3DHistech, Budapest, Hungary) and analyzed with QuPath software (94)*. The Ki67 index was calculated on the whole slide as the number of Ki67-positive cells per total number of cells.* (95)*"*

Surgical procedure:
Operations were performed as described previously (71). "*Briefly, during PVL, ligation of portal branches leading to the right lateral, left part of the median, left lateral, and caudate lobes were performed (70% of the liver). In the case of ALPPS, additional transection was performed alongside the transition line between the left and right part of the median lobe (Figure 5). Liver wounds were sealed carefully by electrocauterization.*

Animals received antibiotic treatment (10 mg/kg body weight metronidazole intraperitoneally) and analgesia (1 mg/kg nalbuphine subcutaneously, repeated once 24 h post-operatively).”(87)

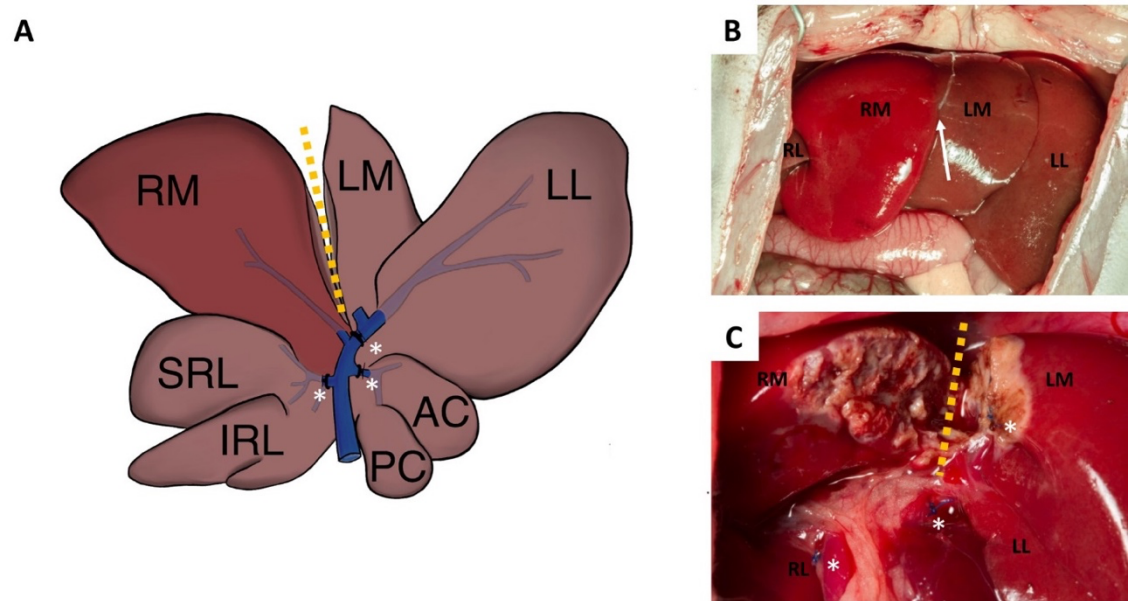

Figure 5. Schematic figure (A) and photographs (B and C) of the operative procedure on rats. Following median laparotomy, in the case of portal vein ligation (PVL), portal branches leading to the superior and inferior right lateral (SRL, IRL), left part of the median (LM), left lateral (LL), and caudate lobes were ligated (*). The non-ligated lobe therefore remained the right median (RM) lobe. In the case of ALPPS, additional transection (yellow dotted line) was performed alongside the transition line (white arrow) between the RM and LM lobes. Figure was adapted without modifications from: Daradics N. et al: Curr Oncol 2021.

Statistical analysis:

Data is expressed as mean ± standard deviation. Normality and homoscedasticity of the data was analyzed with diagnostic tests. Statistical analysis was performed using two-way ANOVA with Tukey’s test for post-hoc analysis, Student's t-test, Mantel-Cox log-rank test and univariable linear regression. For analysis of non-parametric data Mann-Whitney-U test was performed. A p-value ≤ 0.05 was considered statistically significant. Data are presented in mean ± standard deviation (SD). Calculations and visualisation were performed with GraphPad Prism 9 (GraphPad Software Inc., La Jolla).

3.1. Methods of the I. experiment

Male Wistar rats (Toxicoop, Hungary) weighing between 220-250 g were used in the experiment.

3.1.1. Physical prehabilitation protocol and experimental design

"PP protocol was established as previously described (51,71)*. Animals in the PP group received PP one hour long 5 times/week for 5 weeks in form of treadmill running with 16 m/min. The maximum running capacity of the rats – the maximum tolerable speed for 60 minutes without the signs of fatigue – was determined in a preliminary study (20 m/min). During the first week of exercise rats were accustomed to running by 8 m/min speed, which gradually increased each day by 1.6 m/min reaching 80% of the maximum tolerable running speed (16m/min) by the end of the first week. In the following 4 weeks rats continued the exercise with 16 m/min running speed. Animals in the sedentary group were housed in standard conditions for the same time interval (5 weeks) without receiving physical preconditioning.*

Experimental design consisted of three main groups. In experiment 1 (SF 1A) 60 animals were included (n=30 S, n=30 PP). Animals were terminated preoperatively and at 24, 48, 72, 168 h after surgery. Thereafter, liver weight, immunohistochemical and clinical chemistry analyzes were performed. In experiment 2 10 animals were included (n=5 S, n=5 PP). Liver volumetry analyzes MRI and liver function analyzes by 99mTc-mebrofenin hepatobiliary scintigraphy were carried out on the identical animals preoperatively and at 48 and 120 h after surgery. Animals were terminated at the end of the experiment. In experiment 3 36 animals were included (n=18 S, n=18 PP). Animals received LPS injection 24 h following surgery (see 3.1.6.) and the surviving rats were terminated 48 and 192 h after surgery. Thereafter, total blood count test and C-reactive protein measurement was performed. Overall survival and rat grimace scale (RGS) were also determined. (96)*"*

3.1.2. Sample extraction

"Following intraperitoneal injection of 75 mg/kg ketamine and 7.5 mg/kg xylazine in 1.5 mL saline solution the animals were terminated by exsanguination via cardiopuncture. Blood was collected in tripotassium (K3) ethylenediamin tetra-acetic acid (EDTA),

citrate and lithium heparin (Vacutainer) tubes. Following the in toto extraction of the liver, approximately 150 mg tissue of the right median lobe was fixed in 4% buffered formaldehyde for histology. (96)*"*

3.1.3. Magnetic resonance imaging (MRI)-volumetry

"In vivo liver lobe volumes were determined by 3 Tesla (3T) magnetic resonance imaging (MRI) volumetry (coronal T1-weighed gradient echo sequencing, 128 axial slices of 0.4 mm thickness) (nanoScan 3T PET/MRI; Mediso Ltd., Budapest, Hungary). Manual delineation using vivoQuant 1.22 software (inviCRO-Konica-Minolta Inc., Boston, US) of the ligated lobes (LL; right lateral, left part of the median, left lateral, and caudate) and the non-ligated right median lobe, which is equal to the FLR, on each axial slice and three-dimensional reconstruction in a 160x160 matrix was performed. FLRV was expressed as a fraction of total liver volume and body weight. (96)*"*

3.1.4. Laboratory measurements

Plasma AST, ALT, tBil and C-reactive protein level, platelet count, neutrophil percentage (%) and lymphocyte % was measured by Vetlabor Veterinary Clinic and Laboratory (Budapest, Hungary).

3.1.5. 99mTc-mebrofenin hepatobiliary scintigraphy (HBS)

"^{99m}Tc-mebrofenin (combination of Bromo-Biliaron ready-to-use radiopharmaceutical kit (Medi-Radiopharma Ltd., Budapest, Hungary), and ^{99m}Tc isotope solution in physiological saline (Ultra-Technekow Technetium Generator, Mallinckrodt Medical, Petten, Netherlands)), was injected in 140 MBq dosage in 0.13 ml saline into the tail vein. Thereafter, planar HBS (nanoScan SPECT/CT system, Mediso Ltd., Budapest, Hungary) was acquired from four angles in a resolution of 256 x 256 using Ultrahigh Resolution (UHR) parallel septal collimator (Mediso Ltd, Budapest, Hungary). A dynamic protocol of three different phases was used including 12/6/2 frames per minutes for 0.2/2.5/7.0 minutes, respectively, to monitor the rapid uptake and the canalicular elimination of the tracer. Recordings were evaluated with manual allocation of elliptic regions of interest (ROI) to the anteroposterior projection corresponding to the blood pool, as well as the FLR using the Fusion software (Mediso Ltd. Budapest, Hungary). Characteristic

parameters were computed from kinetic curves such as T_{max} and $T_{1/2}$. The uptake of the FLR can be characterized by the midpoint of the ascending section of the curve, which fits well with a linear function. The difference in isotope concentration in the bound lobe and in blood was determined at two time points. This value is then normalized by the applied activity. The washout was determined with same method at the descendent section of the kinetic curve after the inflexion point of the isotope activity curve. (96)*"*

3.1.6. Assessment of postoperative vulnerability

"Postoperative vulnerability was assessed by creating a LPS induced endotoxemia model. LPS (O111:B4, L2630) was purchased from Sigma-Aldrich (St. Louis, Missouri, USA). Rats received intraperitoneal LPS injection (25 mg/body weight kg) 24 h after surgery. Animal survival was determined by consecutive monitoring after LPS injection. Administration of RGS, which features specific facial action units increasing in intensity in response to post-procedural pain (97)*, was performed 4, 12 and 24 h after LPS injection.* (96)*"*

3.1.7. Assessment of body composition

"In vivo fat and muscle volumes were determined by MRI volumetry (coronal T1-weighed gradient echo sequencing, 128 axial slices of 0.4 mm thickness) (nanoScan 3T PET/MRI; Mediso Ltd., Budapest, Hungary). In the first step the subcutaneous and visceral fat were manually roughly segmented using the appropriate size sphere. In the next step for clarification the subcutaneous and visceral fat layer were selected by choosing the density threshold between (10000-18000 voxel greyscale values in vivoQuant 1.22 software (inviCRO-Konica-Minolta Inc., Boston, US)). Total thigh volume was measured at the level of a single vertebral slice (lumbar L3). Measurements were performed in a semi-automated fashion with manual outlining of thigh muscle borders and setting the density.(96)*"*

3.2. Methods of the II. experiment

"Male wild type (WT) BL6/jk (n=30) and CypD knockout (KO) (n=30) mice weighing 22-26 g underwent ALPPS procedure. Mice heterozygous for the gene encoding CypD (originating from the C57Bl6/J strain) were obtained from the Dana-Faber Cancer

Institute. CypD -/- knockout mice were achieved by mating with C57Bl6/F mice in our facilities and afterwards backcrossing with C57Bl6/J mice for at least eight generations to ensure homologous genetic background (Figure 6). (95)*"*

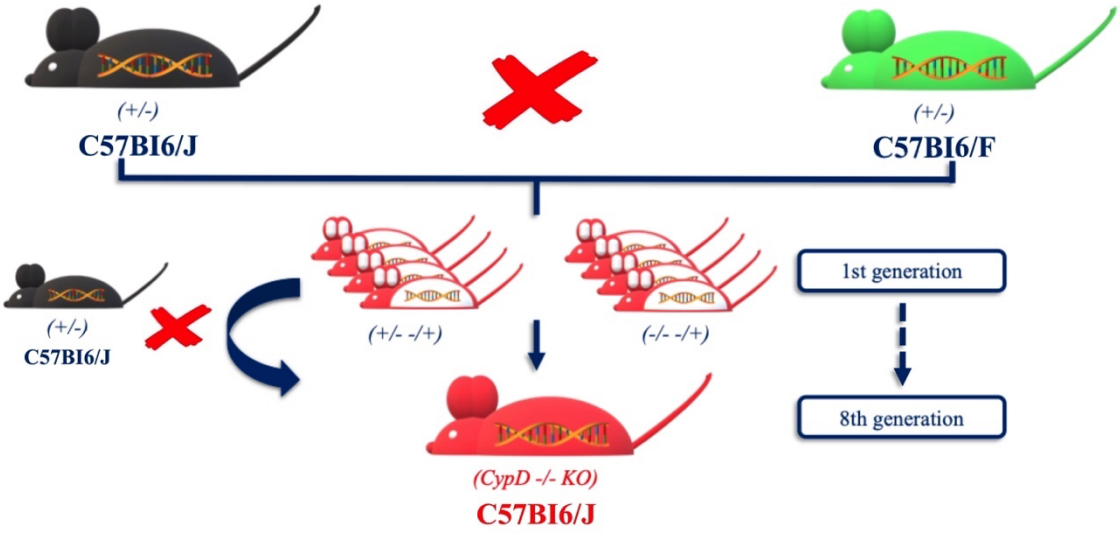

Figure 6. Schematic figure of the generation of Cyclophilin D knockout mice. Cyclophilin D (CypD) -/- knockout mice were achieved by mating mice heterozygous for the gene encoding CypD (originating from the C57Bl6/J strain) with C57Bl6/F mice in our facilities and afterwards backcrossing with C57Bl6/J mice for at least eight generations to ensure homologous genetic background. The figure was created by the author.

3.2.1. Sample extraction

Following 2.5 v/v% with 1 L/min flow isoflurane anaesthesia animals were exsanguinated by cardiopuncture preoperatively and at 24h, 48h, 72h, 168h after surgery. *"Tissue from the non-ligated right median lobe (RML) was snap frozen in liquid nitrogen and stored at -80 °C until further use or fixed in 4% buffered formaldehyde for histology. For the isolation of mitochondria from fresh RML samples discontinuous Percoll gradient was used as described earlier* (98). *Samples were homogenized in isolation buffer A (S1 Table), then centrifuged (3 min x 1300g). Supernatant was removed and centrifuged again (10 min x 20000g) then pellet was suspended in 15% Percoll and layered on a discontinuous gradient consisting of 40 and 23% Percoll layers, which was then centrifuged (8 min x 30700g). The lowermost fraction of isolation buffer was*

resuspended, centrifuged (10 x 16,600g), and the pellet was resuspended and centrifuged again (10 x 6300g). Afterwards the supernatant was discharged, then the pellet was resuspended in isolation buffer. The retrieved pellet containing isolated mitochondria was resuspended in 200 µl isolation medium. Mitochondrial protein content was determined using Pierce™ Coomassie Plus (Bradford) Assay Kit (Thermo Scientific, Waltham, MA). 0.1 mg/ml mitochondrial protein concentration was used throughout the experiments. (95)*"*

3.2.2. Assessment of mitochondrial function

"Mitochondrial ATP synthesis was investigated as previously described (71)*. Incubation medium was supplemented with NADP+ (1.5 mM), hexokinase (2 U/ml), glucose 6-phosphate dehydrogenase (3.84 U/ml), 2.5 mM glucose, and 50 µM P1,P5-di(adenosine-5') pentaphosphate (inhibitor of adenylate kinase). Following coupled enzyme reaction, the absorbance of the reduced nicotinamide adenine dinucleotide phosphate was measured at 340nm (V650 UV/VIS double-beam spectrophotometer, ABL&E Jasco, Tokyo, Japan). ATP production indicating the endogenous substrate supply was assessed in the presence of mitochondria and 2 mM ADP. Stimulated ATP production was evaluated in 5 mM glutamate-malate (GM) (in case of complex I) or 5 mM succinate (in case of complex II) medium.*

As previously reported (51,71)*, oxygen consumption was assessed with an Oxygraph-2K® high resolution respirometry system (Oroboros Instruments, Innsbruck, Austria) by measuring reduced nicotinamide adenine dinucleotide dehydrogenase (I complex) and succinate dehydrogenase (II complex). Basal function (state 4) and induced function stimulated by adenosine 5'-diphosphate (ADP) were measured in GM (complex I) and succinate medium (complex II). Oxygen consumption was adjusted to mitochondrial protein content.*

Intramitochondrial NADP(H) was measured by the autofluorescence of reduced nicotinamide adenine dinucleotide (phosphate) (NAD(P)H) with PTI Deltascan® fluorescence spectrophotometer (Photon Technology International, Lawrenceville, New Jersey, USA) at 37°C, at 344nm excitation and 460nm emission wavelengths. Basal NAD(P)H levels were measured when only mitochondria had been added to the

incubation medium. GM or succinate were added for the measurement of induced production (51,71). (95)*"*

3.2.3. Proteomic analysis of mitochondrial biogenesis, oxidative phosphorylation and apoptosis

"35 mg of liver tissue was homogenized in RIPA buffer (Sigma-Aldrich, St. Louis, MO) by a Bead Beater tissue homogenizer (Next Advance, Inc, Troy, NY). The electrophoresis of samples (20 µg protein/lane) was performed on 8–12 per cent (v/v) sodium dodecyl sulphate–polyacrylamide gels. Protein concentration was measured using Pierce™ Coomassie Plus (Bradford) Assay Kit (Thermo Scientific, Waltham, MA). After transferring proteins on to polyvinylidene difluoride membranes samples were incubated with primary antibodies. Primary antibodies were detected using secondary antibodies (Jackson ImmunoResearch, West Grove, Pennsylvania, USA) and Clarity ECL reagent (Bio-Rad, Hercules, California, USA). Visualization was carried out on Syngene G:Box imager (Syngene, Cambridge, UK) and quantified with FIJI software (99). *Total protein load of the lane served as internal control.* (95)*"*

3.3. Methods of the III. experiment

Male Wistar rats (Toxicoop, Hungary) weighing between 180-220 g were used in the experiment.

3.3.1. Sample extraction

"The animals were sacrificed by exsanguination via cardiopuncture after intraperitoneal injection of 75 mg/kg ketamine and 7.5 mg/kg xylazine in 1.5 mL saline solution. Animal sacrifice was performed at baseline (without any intervention) and 24, 48, 72, or 168 h following PVL and ALPPS (N = 6 per group).

Portal blood was collected into heparinized tubes (Vacutainer) directly before cardiac puncture from the portal vein using a 24 G needle. The remainder of the systemic blood was collected into heparinized tubes by cardiac puncture. The liver and the identical part of the ileum were extracted after sacrifice. Approximately 150 mg tissue from the right median lobe was snap frozen in liquid nitrogen and another 150 mg was fixed in 4%

buffered formaldehyde for histology. Right median lobe samples were snap frozen in liquid nitrogen and stored at -80 °C until further use. (87)*"*

3.3.2. Assessment of hepatic microcirculation and portal pressure

"The microcirculation of the liver was evaluated by laser Doppler flowmetry (LDF) (Moor Instruments, London, UK) during the surgical steps: 5 min after opening of the abdomen (baseline) and 5 min after the ligation of portal branches (in the case of PVL) or the transection (in the case of ALPPS). Individual measurements were performed for 1 min with a surface probe positioned on 3 sites on the right part as well as the left part of the median lobe. A mean value was calculated.

The right portal branch was cannulated with a 24 G needle before sacrifice and an invasive blood pressure monitoring device (model DRT4-3109 Kent Scientific, Torrington, CT, USA) was connected to register portal pressure for 5 min at fixed needle position. Data were recorded with DasyLab software (v9.00.02, National Instruments, Austin, TX, USA).(87)*"*

3.3.3. Quantification of total bile acid concentration

"The total bile acid concentration was determined in heparin-anticoagulated plasma samples with the Total Bile Acids Assay Kit from Diazyme (Poway, CA, USA) using a slightly modified version of the kit manual. In brief, 135 µL of >0.1mM Thio-NAD ('Reagent 1') was added to 4 µL of sample, standard (50 µM conjugated cholic acids), or blank (NaCl) and incubated for 5 min at 37 °C in the dark. Subsequently, 45 µL of 2 kU/L 3-α-HSD/>0.1 mM NADH ('Reagent 2') was added to each well, after which the absorption at 405 nm was read at 2 min-intervals during 12 min on a Synergy HT microplate reader (Biotek, Winooski, VT, USA) at 37 °C. The bile acid concentration was calculated as per manufacturer's instructions. For samples with a high bile acid concentrations, only the data points of the kinetic read over which absorption increased linearly (i.e., with an R^2 of > 0.99) were used for data analysis.(87)*"*

3.3.4. Quantitative real-time polymerase chain reaction (qRT-PCR)

"35 mg of tissue was homogenized in 150 µl of ice cold phosphate buffered saline by using a MagNA Lyser (Roche Applied Sciences, Basel, Switzerland). RNA was isolated

with an RNeasy Mini Kit (Qiagen, Hilden, Germany) and quantified with a NanoDrop (Thermo Fisher Scientific, Waltham, MA). Reverse transcription of 1 µg of mRNA to cDNA was performed using a SensiFAST cDNA Synthesis Kit (Bioline, London, UK) according to the manufacturer's instructions. qRT-PCR was conducted on a LightCycler 480 (Roche) using the SensiFAST SYBR No-ROX mix (Bioline). LinReg software was used to analyze the fluorescence traces [(22)]. Transcript levels of the genes of interest were normalized to those of the housekeeping genes hypoxanthine phosphoribosyltransferase 1 (Hprt1) for ileum samples and the geometric mean of beta-2-microglobulin (B2m) for liver samples. These housekeeping genes proved to be most stable. Primer sequences spanning an intron or exon-exon junction were derived in NCBI Primer Blast. Primer specificity was validated by melting curve analysis and agarose gel electrophoresis.(87)*"*

DOI:10.14753/SE.2023.2809

4. Results

4.1. I. experiment

4.1.1. PP accelerates volumetric liver regeneration

"ALPPS induced liver growth of the FLR both in the sedentary (S) (238.85±27.31 percent) and PP (299.16±16.38 percent) groups, however the increase in liver mass was more expressed in the PP group, resulting in a significant difference between the groups from 48 h until 168 h (Figure 7A, Table 2). Cell proliferation in the FLR also increased in both groups from 24 h to 72 h, reached the peak at 48 h and decreased to the baseline by the end of the experiment. Supporting the increase observed in liver mass, Ki67 index was also higher in the PP group at 48 and 72 h compared to the S group (Figure 7B,D). MRI liver volumetry also showed increased volume of FLR from 48 h to 120 h in the S and PP group, whereby FLRV in the PP group was higher both at 48 and 120 h than in the S group (Figure 7C,E).(96)*"*

DOI:10.14753/SE.2023.2809

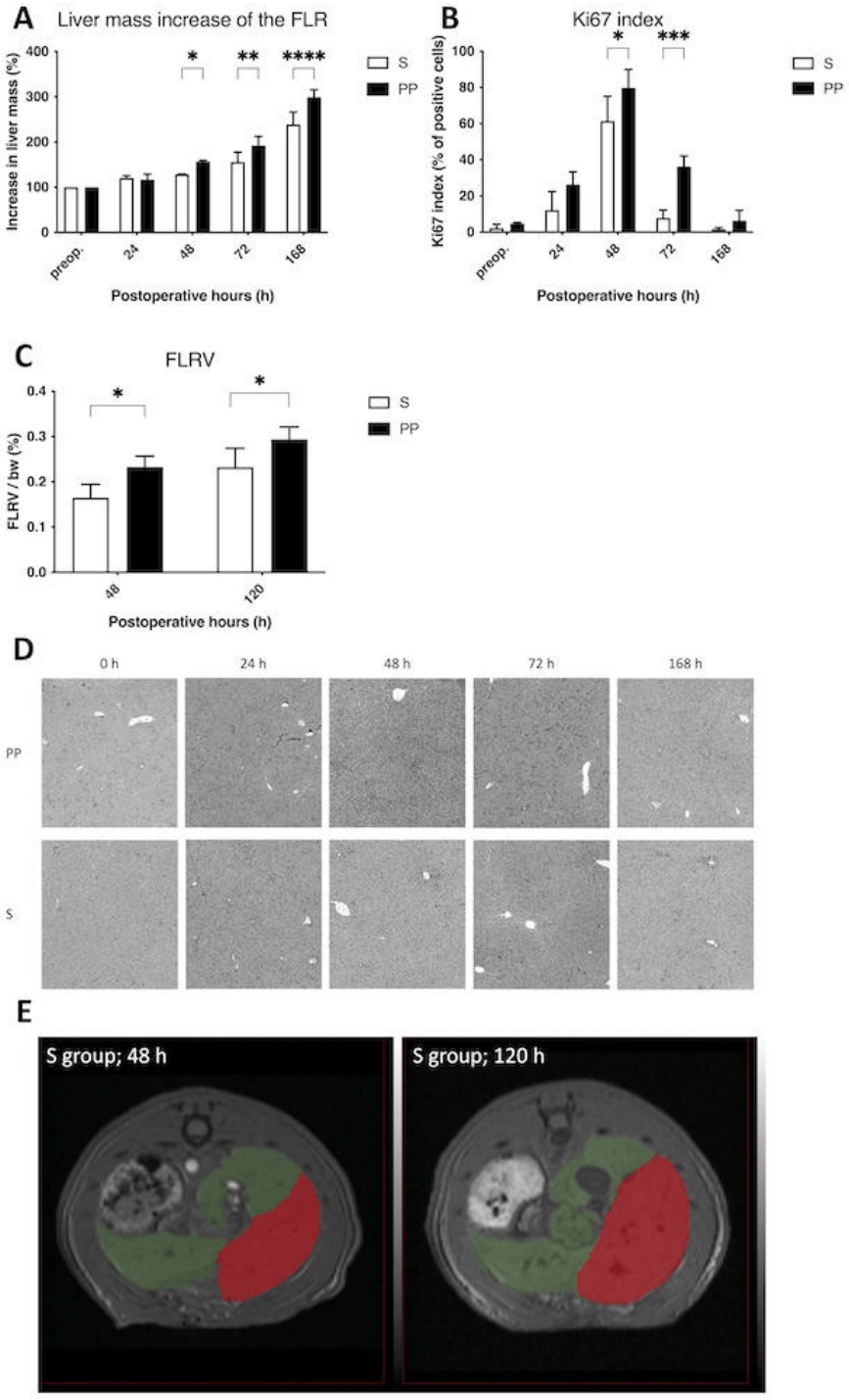

Figure 7. Liver regeneration of the future liver remnant (FLR). Increase in liver mass of the functional liver remnant (FLR) (A) and ki67 index (B, D) preoperatively (preop., 0 h), and at 24 h, 48 h, 72 h, and 168 h after associating liver partition and portal vein ligation for staged hepatectomy (ALPPS) (N = 6 per time point per group). FLR volume (FLRV) (C) at 48 h and 120 h after ALPPS (N = 5 per time point per group). Representative magnetic resonance imaging (MRI)-volumetry picture (E) of volume increase of FLR (red mark) and volume decrease of the

ligated lobes (green mark) in the S group 120 h after ALPPS. * P < 0.050, ** P < 0.0010, *** P < 0.00010, **** P < 0.000010 physical prehabilitation (PP) versus sedentary (S). Figure was adapted without modifications from: Daradics N. et al. Scientific Reports 2022

Table 2. Liver mass increase of the future liver remnant (FLR) in the sedentary and the physical prehabilitation group expressed in mean and standard deviation (SD) at the 24, 48, 72 and 168 postoperative hour.

Postoperative hour	Sedentary (S)		Physical prehabilitation (PP)		p-value
	Increase in liver mass (%)		Increase in liver mass (%)		
	Mean	SD	Mean	SD	
0	100,00	0,00	100,00	0,00	n.s.
24	120,43	4,97	119,89	11,13	n.s.
48	125,04	2,17	155,84	2,11	p < 0.050
72	148,87	19,86	198,15	17,84	p < 0.0010
168	229,55	20,46	305,22	7,74	p < 0.000010

4.1.2. PP ameliorates liver function laboratory parameters after ALPPS

"The level of ALT increased significantly at 24 h in the S group and abated towards baseline level by the end of the experiment, while in the PP group the increase was less explicit. Therefore, ALT level was significantly lower in the PP group at 24 h (Figure 8A). AST level changed by the same dynamic, as it sharply peaked in the S group at 24 h and remained lower in the PP group during the experiment resulting in a disparity between the groups at 24 h (Figure 8B). Similarly, total bilirubin (tBil) level increased in the S group at 24 h and decreased by the end of the experiment, while there was no change in the PP group. Consequently, tBil level was significantly lower in the PP group compared to the S group at 24 h (Figure 8C). (96)"

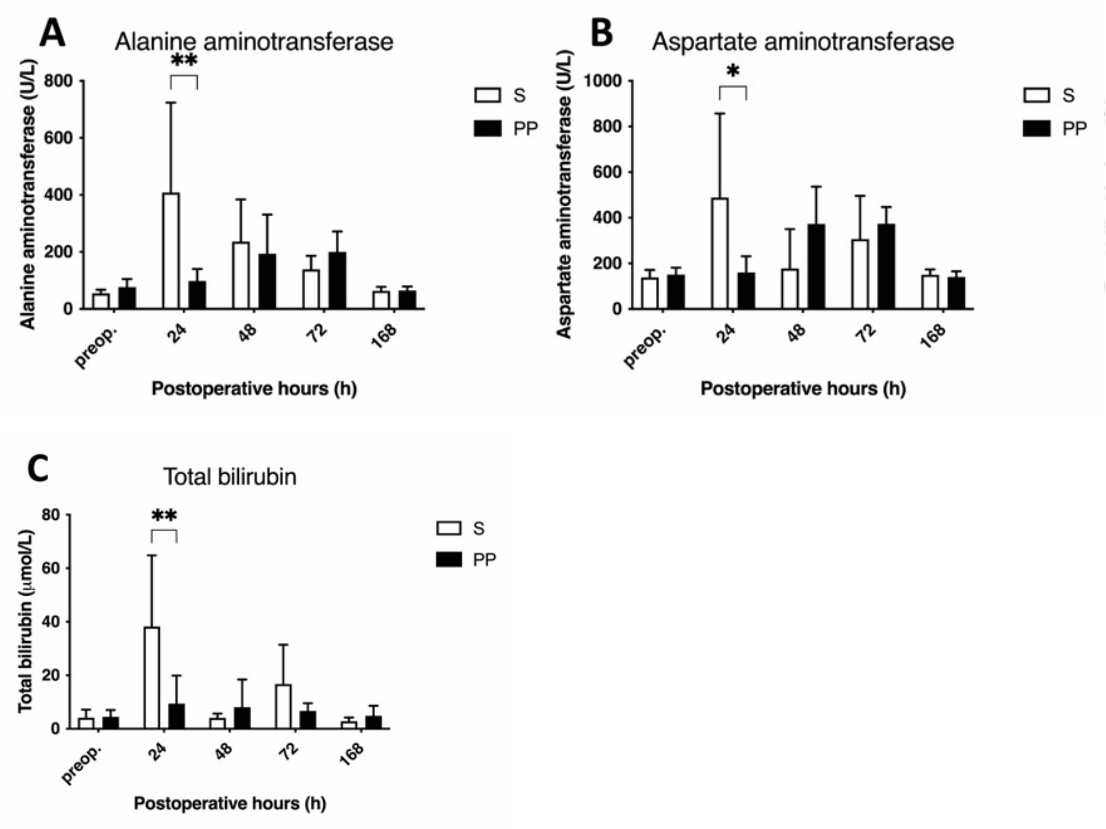

Figure 8. Changes in liver function laboratory parameters. Level of alanine aminotransferase (A), aspartate aminotransferase (B) and total bilirubin (C) preoperatively (preop., 0 h), and at 24 h, 48 h, 72 h, and 168 h after associating liver partition and portal vein ligation for staged hepatectomy (ALPPS) (N = 6 per time point per group). * $P < 0.050$, ** $P < 0.0010$ physical prehabilitation (PP) versus sedentary (S). Figure was adapted without modifications from: Daradics N. et al. Scientific Reports 2022

4.1.3. PP improves liver function measured by ^{99m}Tc-mebrofenin HBS after ALPPS

"T_{max}, which characterizes the organic anion uptake capacity of the liver, did not show difference between the S and PP group (Figure 9A). By the same token, there was no significant disparity in ^{99m}Tc-mebrofenin uptake between the groups (Figure 9B). However, $T_{1/2}$ was significantly lower at 48 h in the PP group compared to the S group, indicating a more effective hepatic excretion after ALPPS in the PP group (Figure 9C). Supporting this, ^{99m}Tc-mebrofenin washout was significantly higher in the PP group compared to the S group at 48 h (Figure 9D), too. (96)*"*

DOI:10.14753/SE.2023.2809

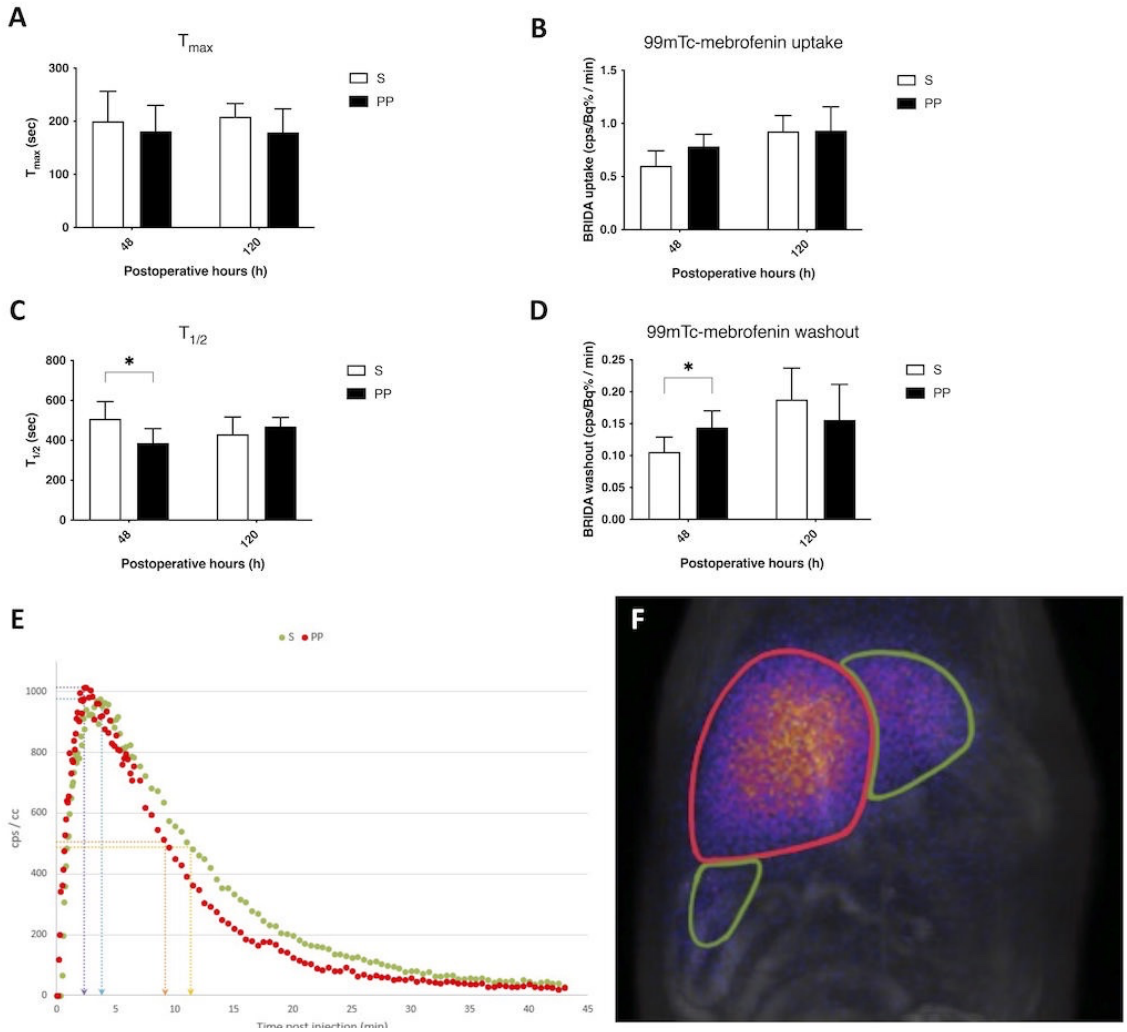

Figure 9. Changes in liver function measured by 99mTc-mebrofenin hepatobiliary scintigraphy (HBS). Time of maximum (T_{max}) 99mTc-mebrofenin concentration (A), total 99mTc-mebrofenin uptake (B), tracer half-life ($T_{1/2}$) 99mTc-mebrofenin concentration and total 99mTc-mebrofenin washout (D) preoperatively (preop., 0 h), and at 24 h, 48 h, 72 h, and 168 h after associating liver partition and portal vein ligation for staged hepatectomy (ALPPS) (N = 6 per time point per group). Representative curve of 99mTc-mebrofenin concentration in the change of time (E) with T_{max} of the PP group (purple arrow), T_{max} of the S group (blue arrow), $T_{1/2}$ of the PP group (orange arrow) and $T_{1/2}$ of the S group (yellow arrow). Representative figure of 99mTc-mebrofenin HBS 48 h after ALPPS in the PP group (F) showing a notable difference of 99mTc-mebrofenin uptake between the functional liver remnant (FLR) and the ligated lobes . * $P < 0.050$, ** $P < 0.0010$ physical prehabilitation (PP) versus sedentary (S). Figure was adapted without modifications from: Daradics N. et al. Scientific Reports 2022

4.1.4. PP mitigates vulnerability in the LPS endotoxemia model after ALPPS

"Vulnerability of the animals was assessed after the operation by inducing endotoxemia with LPS injection. A notable difference could be observed between the two groups, as the survival rate after LPS injection was 91.67 percent in the PP group, while only 41.67 percent in the S group, indicating an excessively increased stress-tolerance in the PP animals (Figure 10A). Underpinning this, the RGS showed significantly lower values in the PP group compared to the S group, suggesting reduced pain in the PP animals after LPS injection (Figure 10B). In line with the above, laboratory results also showed better stress-tolerance in the PP group, as the CRP level was higher (Figure 10C), platelet count lower (Figure 10D), neutrophil % higher (Figure 10E) and lymphocyte % lower (Figure 10F) in the S animals compared to the PP group, indicating markedly expressed inflammation, thrombocytopenia, neutrophilia and lymphocytopenia in the sedentary animals.(96)*"*

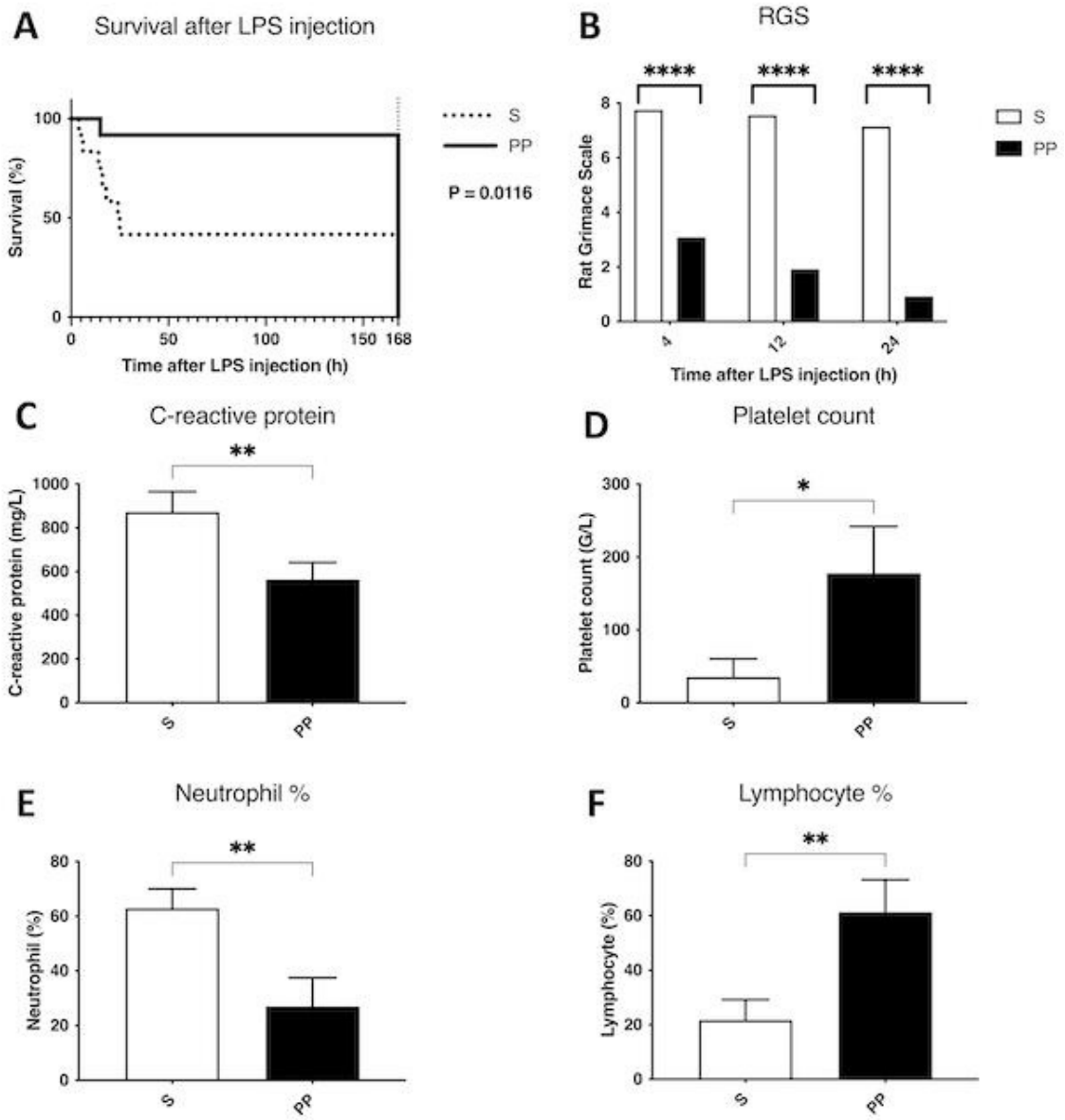

Figure 10. Changes in the vulnerability of the animals in lipopolysaccharide (LPS) endotoxemia model. Survival after LPS injection following associating liver partition and portal vein ligation for staged hepatectomy (ALPPS) monitored for 168 h (A). Rat Grimace Scale (RGS) monitored at 4 h, 12 h and 24 h after LPS injection utilized following associating liver partition and portal vein ligation for staged hepatectomy (ALPPS) (B). C-reactive protein (C), platelet count (D), neutrophil percent (%) (E) and lymphocyte % (F) monitored at 24 h after LPS injection utilized following associating liver partition and portal vein ligation for staged hepatectomy (ALPPS). * $P < 0.050$, ** $P < 0.0010$, **** $P < 0.00001$ physical prehabilitation (PP) versus sedentary (S) (N = 6 per time point per group). Figure was adapted without modifications from: Daradics N. et al. Scientific Reports 2022

4.1.5. PP ameliorates body composition, which correlates with volumetric regeneration after ALPPS

"Confirming that exercise was properly implemented, the body fat composition of the animals in the PP group improved, as the percentage of both visceral (Figure 11A) and subcutaneous (Figure 11B) fat was reduced in the PP group compared to the S group on the preoperative MRI. There was no significant difference between the two group regarding muscle volume (Figure 11C).
On univariable linear regression analysis, the subcutaneous fat percentage correlated with FLRV at 48 h, while only a tendentious correlation could be observed at 120 h (Figure 11D-E). No correlations were found between either visceral fat percentage and FLRV, nor subcutaneous or visceral fat percentage and T_{max}, $T_{1/2}$, ^{99m}*Tc-mebrofenin uptake and* ^{99m}*Tc-mebrofenin washout.* (96)*"*

DOI:10.14753/SE.2023.2809

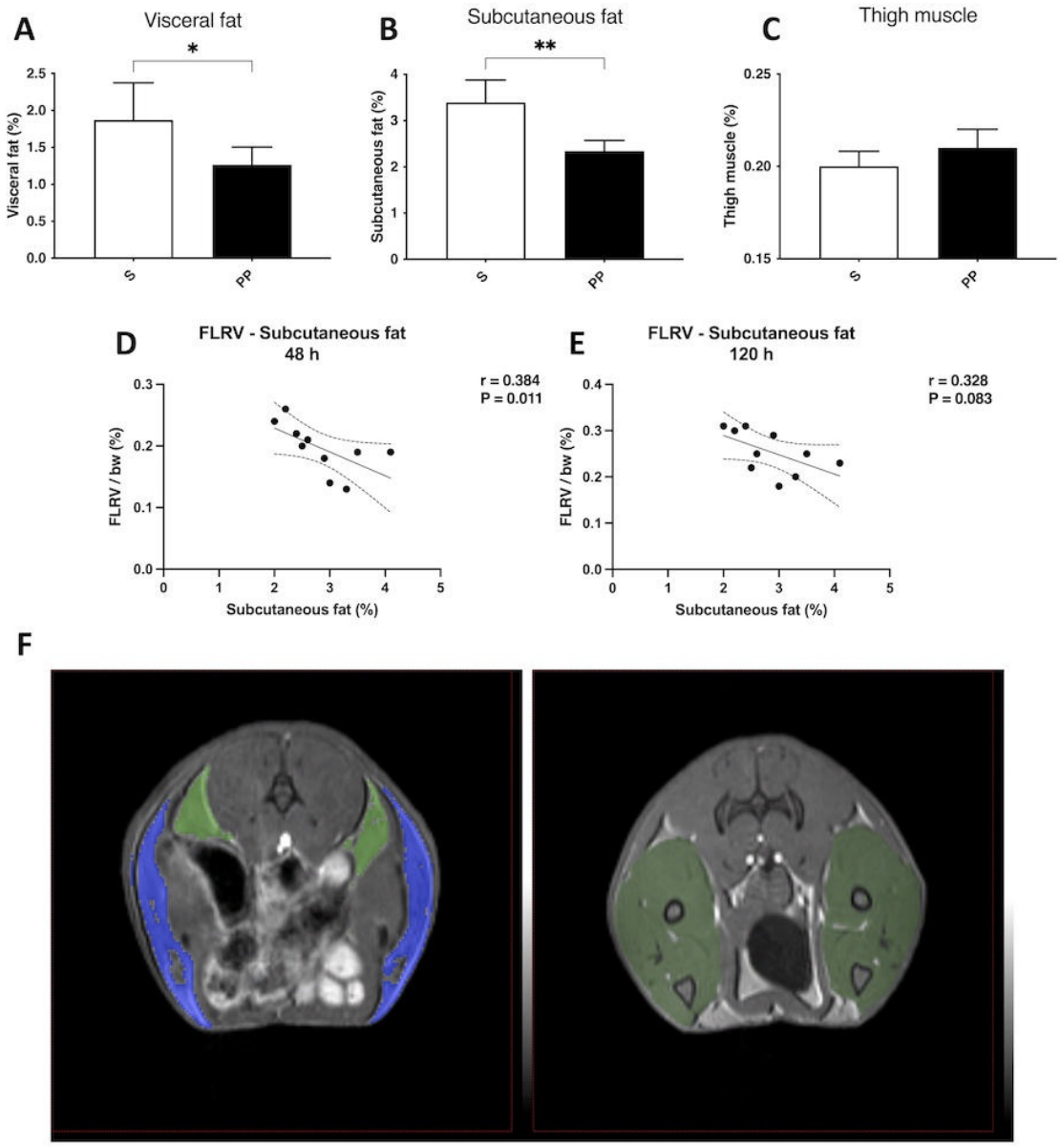

Figure 11. Preoperative magnetic resonance imaging (MRI)-volumetry of body composition and correlation between subcutaneous fat and future liver remnant volume (FLRV). Changes in preoperative visceral fat (A), subcutaneous fat (B) and thigh muscle (C) mass. Linear regression analysis of correlation between subcutaneous fat and FLRV at 48 h (D) and 120 h (E) after associating liver partition and portal vein ligation for staged hepatectomy (ALPPS). Representative figure of preoperative MRI-volumetry (F) of the subcutaneous fat (blue), visceral fat (light green) and thigh muscle (dark green) in the PP group. * $P < 0.050$, ** $P < 0.0010$ physical prehabilitation (PP) versus sedentary (S). Figure was adapted without modifications from: Daradics N. et al. Scientific Reports 2022

DOI:10.14753/SE.2023.2809

4.2. II. experiment

4.2.1. Depletion of CypD enhances mitochondrial function following ALPPS

"Although mitochondrial function showed a significant decrease in the wild type (WT) group following ALPPS in the first 24-48 h, which is in accordance with our previous results (51,71)*, it remained preserved overall in the CypD KO group during this time interval. Mitochondrial function was investigated using the parameters described below.* (95)*"*

4.2.1.1. Depletion of CypD preserves adenosine-5'-triphosphate (ATP) production

"As presented in Figure 12A-B, ALPPS resulted in a decrease of ATP production of endogenous substrates from 24 h until 168 h in the WT group, while it was preserved in the CypD KO group at 24 hour and decreased only after from 48 h to 168 h, marking a significant difference between the groups. Stimulated ATP production of complex I showed conjointly a drop at 24 h in the WT group in opposition with preserved value s in the CypD KO group (Figure 12C-D). (95)*"*

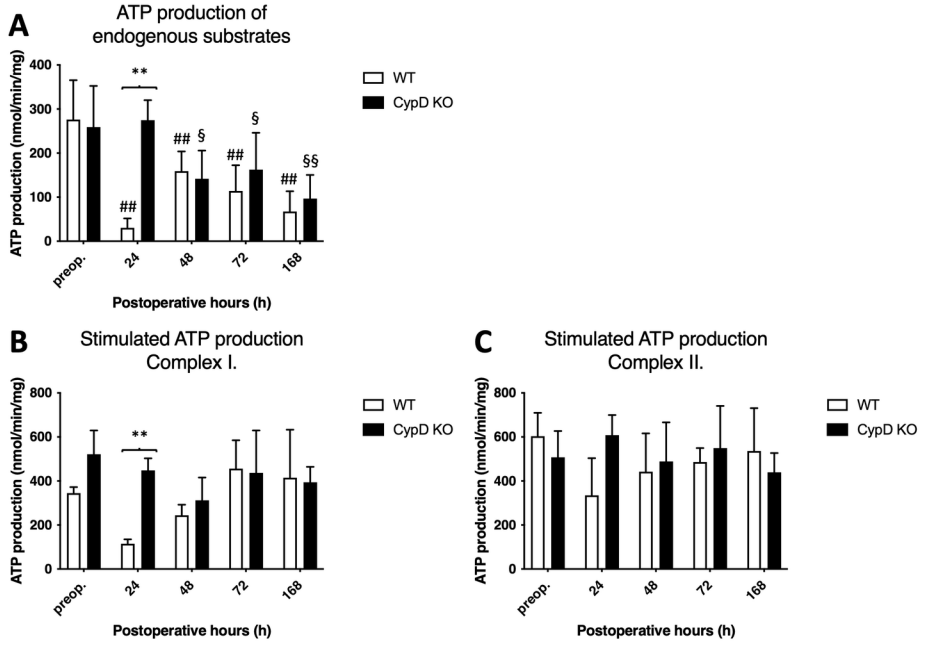

Figure 12. Alterations of adenosine 5′ -triphosphate (ATP) production. Endogenous (A) and exogenous substrate (complex I: glutamate-malate complex II: succinate) stimulated (B and C) ATP production preoperatively (preop., 0 h), and at 24 h, 48 h, 72 h, and 168 h after Associating Liver Partition and Portal vein ligation for Staged hepatectomy (ALPPS) (N = 6 per time point per group). * P < 0.050, ** P < 0.0010 versus wild type (WT); # P < 0.050, ## P < 0.001 WT versus corresponding controls (preop.); § P < 0.050, §§ P < 0.0010 CypD KO versus corresponding controls (preop.). Statistical analysis was performed with a two-way ANOVA and Tukey's post hoc test. Figure was adapted without modifications from: Daradics N. et al. Plos One 2022

4.2.1.2. Depletion of CypD enhances oxygen consumption

"Basal oxygen consumption remained similar to the preoperative value in the WT group, with a temporary increase of complex I at 48 h. In contrast, CypD KO group peaked at 24 h gradually normalizing by the end of the experiment (Figure 13A-B). This resulted in a notably higher oxygen consumption at 24 h in the CypD KO group compared to the WT group. Induced oxygen consumption increased in complex I at 48 and 168 h, while in complex II from 48 h to 168 h in the WT group.

In the CypD KO group complex II showed an earlier increase from 24 h to 72 h, which is line with the energy demanding processes following ALPPS (51)*. This resulted in a*

significantly increased induced oxygen consumption in the CypD KO group compared to the WT group at 24-48 h, in the most energy-consuming phase of liver regeneration following ALPPS (Figure 13C-D) (29). (95)*"*

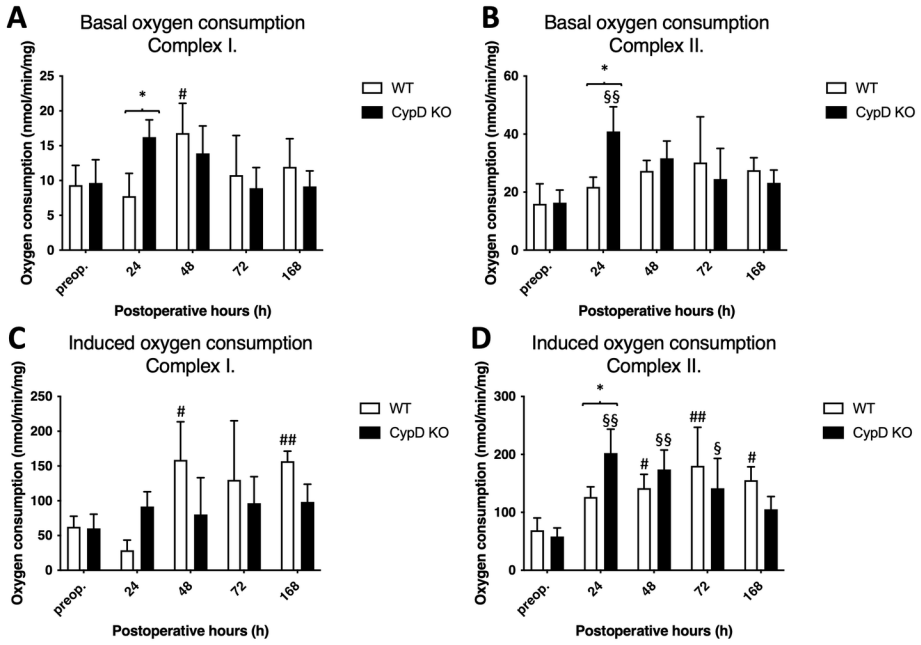

Figure 13. Changes in oxygen consumption levels. Basal (A and B) and substrate (complex I: glutamate-malate complex II: succinate) induced (C and D) oxygen consumption preoperatively (preop., 0 h), and at 24 h, 48 h, 72 h, and 168 h after Associating Liver Partition and Portal vein ligation for Staged hepatectomy (ALPPS) (N = 6 per time point per group). * $P < 0.050$, ** $P < 0.0010$ versus WT; # $P < 0.050$, ## $P < 0.001$ wild type (WT) versus corresponding controls (preop.); § $P < 0.050$, §§ $P < 0.0010$ CypD KO versus corresponding controls (preop.). Statistical analysis was performed with a two-way ANOVA and Tukey's post hoc test. Figure was adapted without modifications from: Daradics N. et al. Plos One 2022.

4.2.2. Depletion of CypD does not alter intramitochondrial nicotinamide adenine dinucleotide phosphate (NAD(P)H) content

"Our previous results revealed that following ALPPS NAD(P)H content decreases (51)*. In line with this, basal concentration of NAD(P)H in the WT group decreased at 24 h in complex I and from 24 h to 168 h in complex II. Corresponding changes could be observed in the CypD KO group, as basal concentration decreased at 24 h and 168 h in complex I and at 168 h in complex II. Therefore, there was no significant difference*

between the two groups regarding basal NAD(P)H concentration (Figure 14A-B). Induced NAD(P)H concentration changed similarly to the basal concentration. A decrease could be observed in the WT group at 24 h in complex I, with no change in complex II. Induced concentration also decreased in the CypD group 24, 72, and 168 h following surgery in complex I, while remained unchanged in complex II. Likewise, there was no difference between the induced NAD(P)H concentration of the two groups (Figure 14C-D). (95)*"*

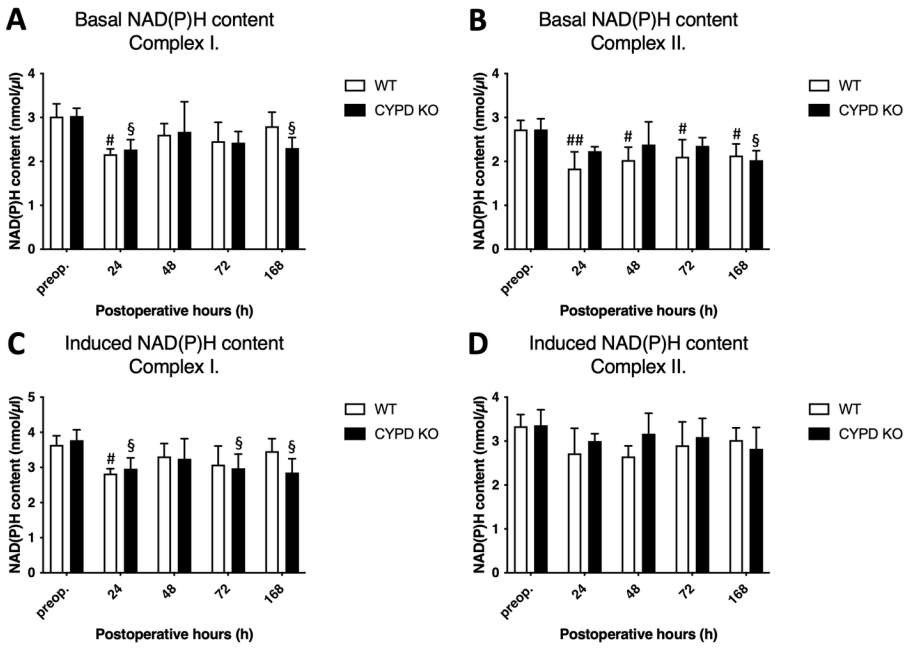

Figure 14. Changes in reduced nicotinamide adenine dinucleotide (phosphate) (NAD(P)H) content. Basal (A and B) and substrate (complex I: glutamate-malate complex II: succinate) induced (C and D) NAD(P)H preoperatively (preop., 0 h), and at 24 h, 48 h, 72 h, and 168 h after Associating Liver Partition and Portal vein ligation for Staged hepatectomy (ALPPS) (N = 6 per time point per group). * $P < 0.050$, ** $P < 0.0010$ versus wild type (WT); # $P < 0.050$, ## $P < 0.001$ WT versus corresponding controls (preop.); § $P < 0.050$, §§ $P < 0.0010$ CypD KO versus corresponding controls (preop.). Statistical analysis was performed with a two-way ANOVA and Tukey's post hoc test. Figure was adapted without modifications from: Daradics N. et al. Plos One 2022.

4.3. Depletion of CypD increases mitochondrial biogenesis coordinator PGC1-α level

"ALPPS caused the decrease of the mitochondrial biogenesis coordinator PGC1-α at 72 and 168 h in the WT group, which is in accordance with our previous results (51)*. On the other hand, CypD depletion increased the level of PGC1-α, as it was found elevated in the CypD KO group from 48h until the end of the experiment. This resulted in a notable difference between the groups from 48 h to 168 h (Figure 15A). Despite of the changes in PGC1-α, NRF 1 level did not change significantly neither in the WT, nor in the CypD KO group (Figure 15B).* (95)*"*

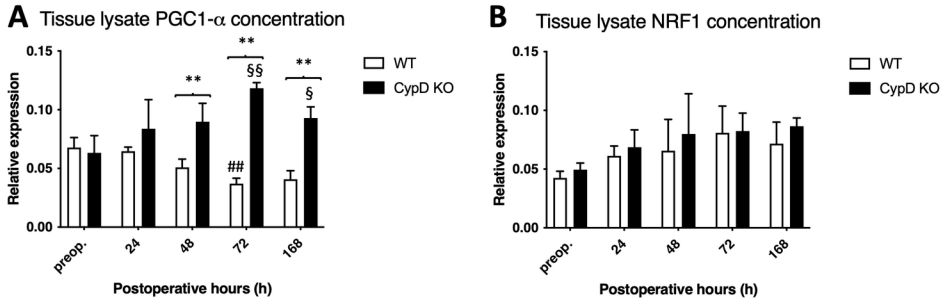

Figure 15. Expression of gene regulatory proteins participating in mitochodrial biogenesis. Peroxisome proliferator-activated receptor γ coactivator (PGC) 1-α (A), nuclear respiratory factor 1 (B) preoperatively (preop., 0 h), and at 24 h, 48 h, 72 h, and 168 h after Associating Liver Partition and Portal vein ligation for Staged hepatectomy (ALPPS) (N = 6 per time point per group). * P < 0.050, ** P < 0.0010 versus wild type (WT); # P < 0.050, ## P < 0.001 WT versus corresponding controls (preop.); § P < 0.050, §§ P < 0.0010 CypD KO versus corresponding controls (preop.). Statistical analysis was performed with a two-way ANOVA and Tukey's post hoc test. Figure was adapted without modifications from: Daradics N. et al. Plos One 2022.

4.2.4. Depletion of CypD increases oxidative phosphorylation system (OXPHOS) protein levels

"In the WT group OXPHOS complex I-III levels did not change significantly throughout the experiment, while in case of complex IV a temporary increase could be observed at 72 h. Similarly, OXPHOS complex I-IV levels in the CypD KO group did not change during the experiment. However, due to an initially higher level at the baseline, level of OXPHOS complex I the CypD KO group was higher compared to the WT group

preoperatively and at 24 h, in case of complex II the same disparity could be observed at 48 h, at the most vulnerable time points following ALPPS (Figure 16A-D). (95)*"*

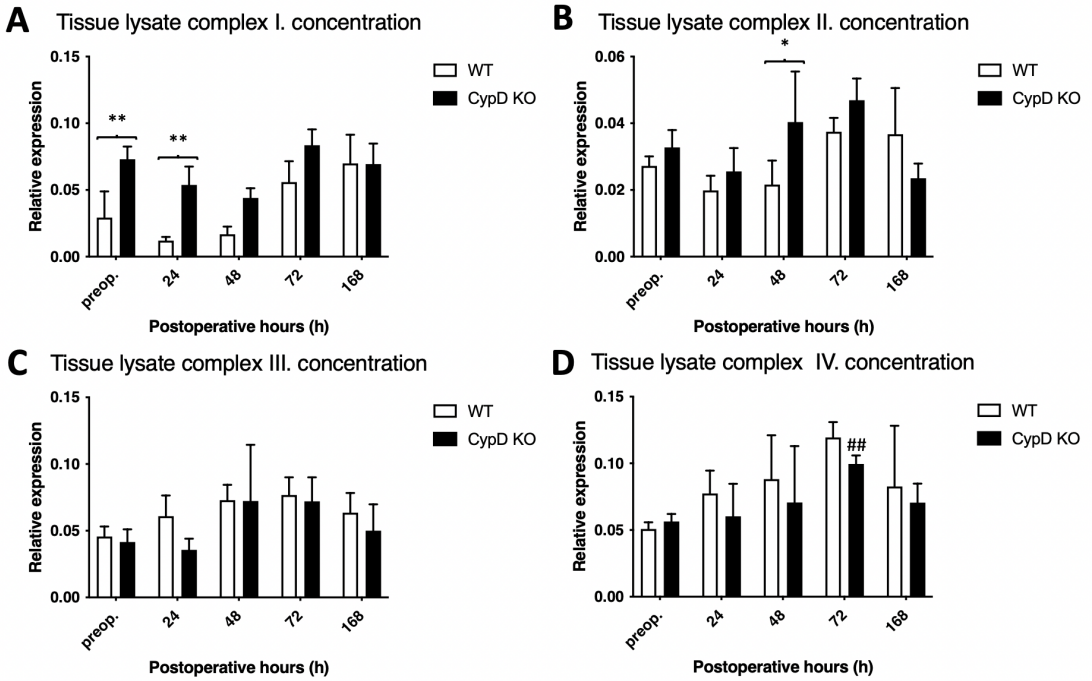

Figure 16. Changes in the expression of the respiratory chain complexes. Complex I (A), complex II (B), complex III (C), complex IV (D) total cell lysate protein concentrations preoperatively (preop., 0 h), and at 24 h, 48 h, 72 h, and 168 h after Associating Liver Partition and Portal vein ligation for Staged hepatectomy (ALPPS) (N = 6 per time point per group). * $P < 0.050$, ** $P < 0.0010$ versus wild type (WT); # $P < 0.050$, ## $P < 0.001$ WT versus corresponding controls (preop.); § $P < 0.050$, §§ $P < 0.0010$ CypD KO versus corresponding controls (preop.). Statistical analysis was performed with a two-way ANOVA and Tukey's post hoc test. Figure was adapted without modifications from: Daradics N. et al. Plos One 2022.

4.2.5. Depletion of CypD alters activation of apoptotic caspase-3

"The level of uncleaved proenzyme form of caspase-3 did not change in the WT group, while a significant increase could be observed from 48 h until the end of the experiment in the CypD KO group (Figure 17A). The level of the activated cleaved form of caspase-3 was elevated at 24 h in the WT group and remained increased by the end of the experiment, which is in line with previous results on apoptotic activity following ALPPS.

In contrast, active caspase-3 level in the CypD KO group increased significantly only from 72 h to168 h, in the remodeling period of ALPPS (Figure 17B). (95)*"*

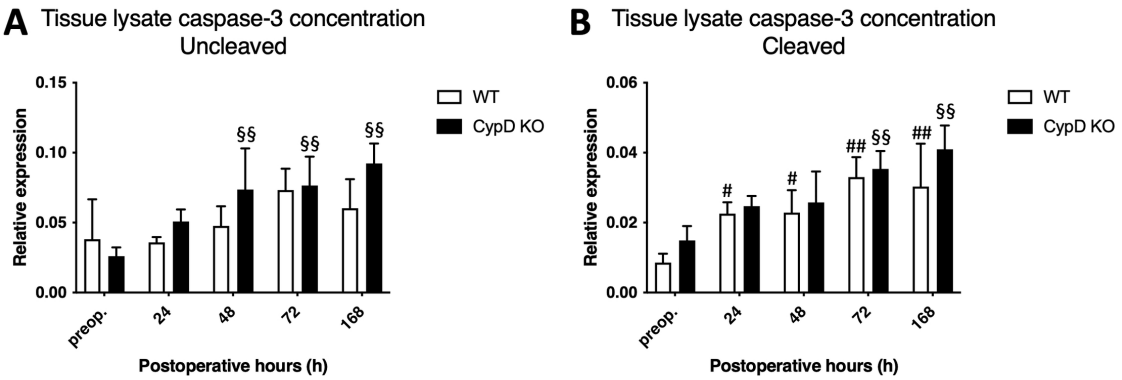

Figure 17. Expression of caspase-3. Uncleaved (A) and cleaved (B) caspase-3 total cell lysate protein concentrations preoperatively (preop., 0 h), and at 24 h, 48 h, 72 h, and 168 h after Associating Liver Partition and Portal vein ligation for Staged hepatectomy (ALPPS) (N = 6 per time point per group). * $P < 0.050$, ** $P < 0.0010$ versus wild type (WT); # $P < 0.050$, ## $P < 0.001$ WT versus corresponding controls (preop.); § $P < 0.050$, §§ $P < 0.0010$ CypD KO versus corresponding controls (preop.). Statistical analysis was performed with a two-way ANOVA and Tukey's post hoc test. Figure was adapted without modifications from: Daradics N. et al. Plos One 2022.

4.2.6. Depletion of CypD accelerates liver growth and cell proliferation

"Both in the WT and CypD KO groups, liver mass gradually increased. However, while liver growth achieved only about 100% growth in the WT group, the CypD KO group displayed a 150% growth, resulting significantly higher liver mass in the CypD KO group at 168 h compared to the WT group (Figure 18A, Table 3). Mitotic rate and ki67 index in both WT and CypD KO group increased until 48 h, after which the cell division gradually normalized by the end of the experiment. No difference could be observed nor between the mitotic rates either the ki67 index of the groups (Figure 18B, C). (95)*"*

DOI:10.14753/SE.2023.2809

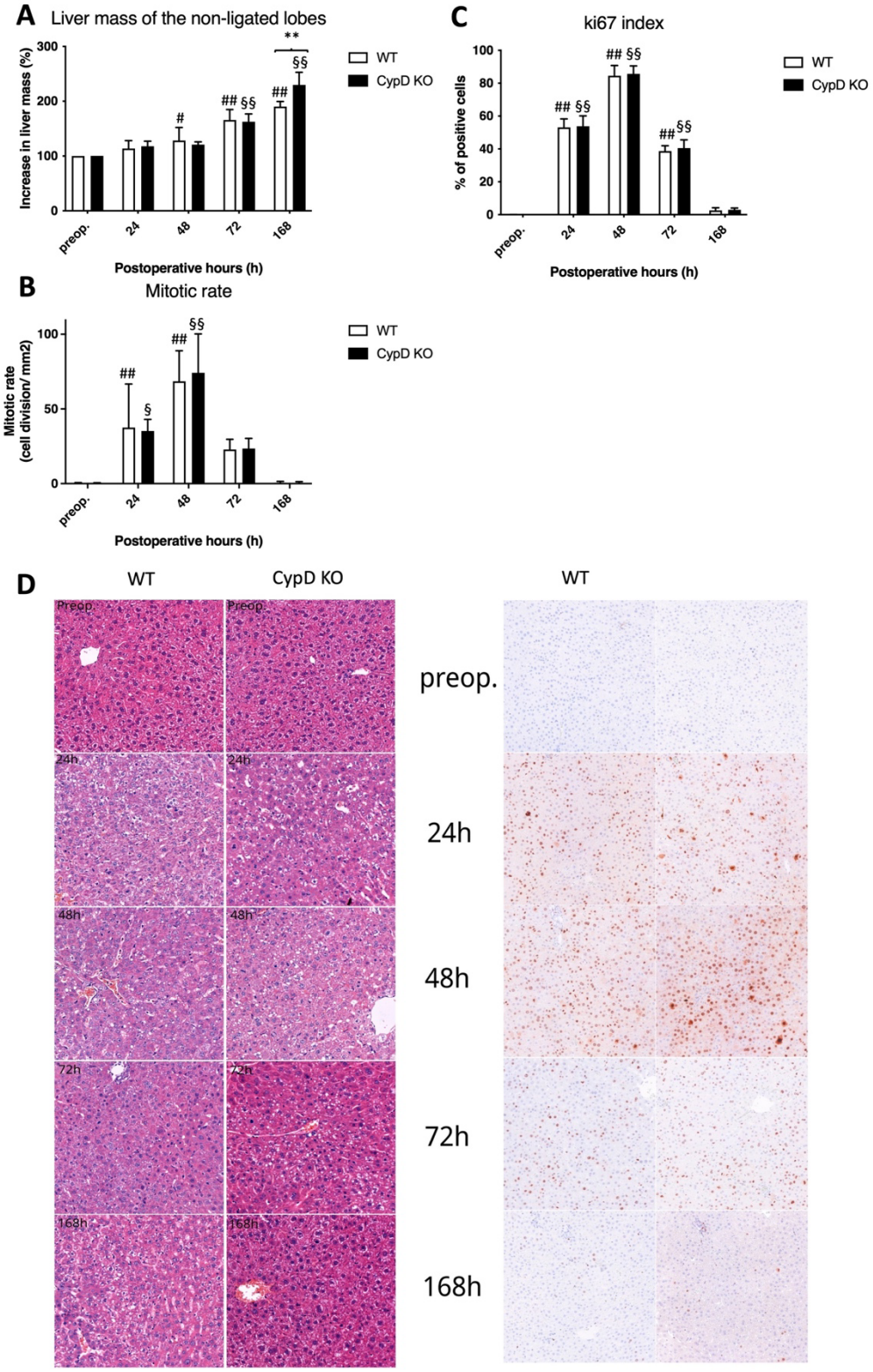

Figure 18. Liver regeneration following Associating Liver Partition and Portal vein ligation for Staged hepatectomy (ALPPS) in the ligated right medial lobe. Increase in liver mass of non-ligated lobe (A) and mitotic rate (B) and ki67 index (C) preoperatively (preop., 0 h), and at 24 h, 48 h, 72 h, and 168 h after ALPPS (N = 6 per time point per group). Histological structure on the left (hematoxylin and eosin stain; original magnification: ×150) and ki67 immunohistochemistry (on the right) of the regenerating right median (RM) lobe (D) preoperatively (preop.) and at 24 h, 48 h, 72 h, and 168 h after ALPPS in the Cyclopihilin D knockout (CypD KO) and wild type (WT) group. * $P < 0.050$, ** $P < 0.0010$ versus wild type (WT); # $P < 0.050$, ## $P < 0.001$ WT versus corresponding controls (preop.); § $P < 0.050$, §§ $P < 0.0010$ CypD KO versus corresponding controls (preop.). Statistical analysis was performed with a two-way ANOVA and Tukey's post hoc test. Figure was adapted without modifications from: Daradics N. et al. Plos One 2022.

Table 3. Liver mass increase of the right median lobe in the wild type (WT) and the Cyclophilin D knockout (CypD KO) group expressed in mean and standard deviation (SD) at the 24, 48, 72 and 168 postoperative hour.

Postoperative hour	Wild type (WT)		Cyclophilin D knockout (CypD KO)		p-value
	Increase in liver mass (%)		Increase in liver mass (%)		
	Mean	SD	Mean	SD	
0	100,00	0,00	100,00	0,00	n.s.
24	113,86	14,18	114,44	11,46	n.s.
48	128,36	23,70	115,58	13,22	n.s.
72	165,85	19,00	162,41	14,31	n.s.
168	190,48	9,03	229,58	23,16	$p < 0.0010$

DOI:10.14753/SE.2023.2809

4.3. III. experiment

4.3.1. Accelerated liver regeneration and cell proliferation following ALPPS

"Both PVL and ALPPS induced growth of the right part of the median lobe from 24 h to 168 h (Figure 19A, Table 4), whereby an increase in liver mass of the non-ligated lobes was higher in the ALPPS group compared to the PVL group at all time points. Cell proliferation in the non-ligated lobes in both groups was higher from 24 h to 72 h versus baseline and abated towards baseline levels at the end of the experiment (Figure 19B,C). The Ki67 index in the right part of the median lobe was higher in the ALPPS group compared to the PVL group at 24 h and 48 h. (87)*"*

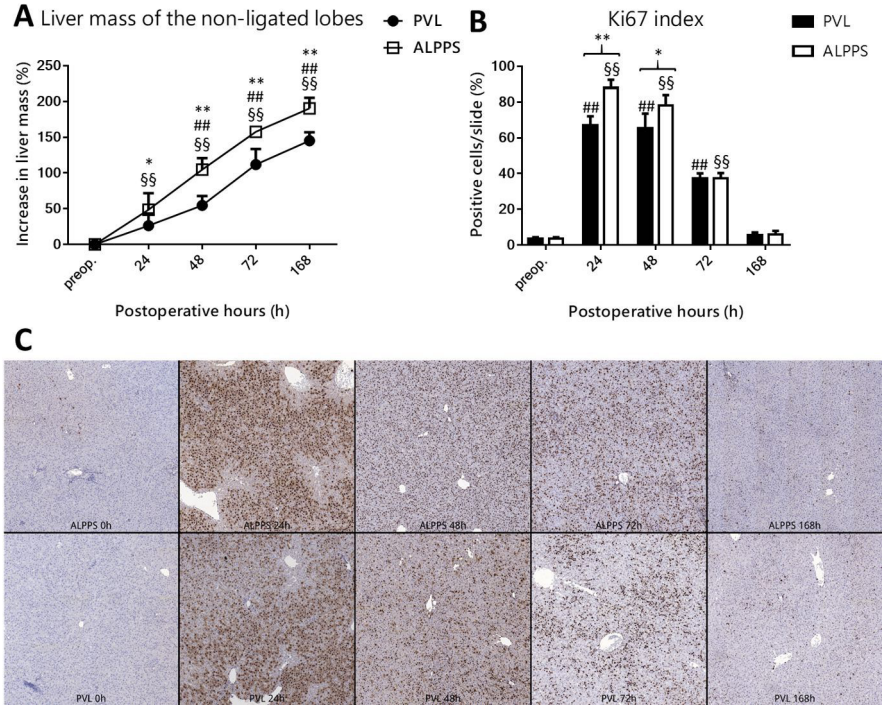

Figure 19. Effect of portal vein ligation (PVL) and associating liver partition and portal vein ligation for staged hepatectomy (ALPPS) on right medial lobe mass and hepatocellular proliferation. Increase in liver mass of non-ligated lobe (A) and Ki67 index (B, C) preoperatively (preop., 0 h), and at 24 h, 48 h, 72 h, and 168 h after PVL and ALPPS (n = 6 per time point per group). * $p < 0.050$, ** $p < 0.0010$ versus PVL; ## $p < 0.001$ PVL versus corresponding controls (preop.); §§ $p < 0.0010$ ALPPS versus corresponding controls (preop.). Statistical analysis was performed with a two-way ANOVA and Tukey's post hoc test. Data are presented as mean ± 1

standard deviation (SD). Figure was adapted without modifications from: Daradics N. et al: Curr Oncol 2021.

Table 4. Liver mass increase of the non-ligated lobes in the portal vein ligation (PVL) and associating liver partition and portal vein ligation for staged hepatectomy (ALPPS) group expressed in mean and standard deviation (SD) at the 24, 48, 72 and 168 postoperative hour.

Postoperative hour	PVL		ALPPS		p-value
	Increase in liver mass (%)		Increase in liver mass (%)		
	Mean	SD	Mean	SD	
0	100,00	0,00	100,00	0,00	n.s.
24	117,50	27,57	148,63	23,24	$p < 0.050$
48	154,78	12,94	204,67	16,10	$p < 0.0010$
72	211,79	21,83	257,52	7,03	$p < 0.0010$
168	245,07	11,96	290,35	14,81	$p < 0.0010$

4.3.2. Decrease in liver microcirculation in the ligated lobes after ALPPS

"Contrived occlusion of blood supply to portions of the liver causes a divergence of blood flow between the ligated and the non-ligated liver segments. In line with this, both PVL and ALPPS resulted in an increase in microcirculatory flow in the right median lobe while flow in the ligated left median lobe had decreased compared to the pre-ligation flow (Figure 20A). The transection part of ALPPS exerted no additional effect on flow in the non-ligated right median lobe but further decreased flow in the ligated left median lobe. (87)*"*

4.3.3. Portal pressure increases following ALPPS

"Both interventions were associated with an increase in portal pressure immediately and at 24 h post-intervention, after which the pressure gradually normalized by the end of the

experiment (Figure 20B). These findings are consistent with the fact that an equal amount of blood is directed into the smaller liver volume after PVL and support the microvascular flow data. Compared to baseline, the portal pressure remained elevated for 48 h in the PVL group and for 72 h in the ALPPS group. At 168 h after the intervention the portal pressure had reverted to baseline level. The increase in portal pressure was greater in the ALPPS group compared to the PVL group during the first 24 h. (87)*"*

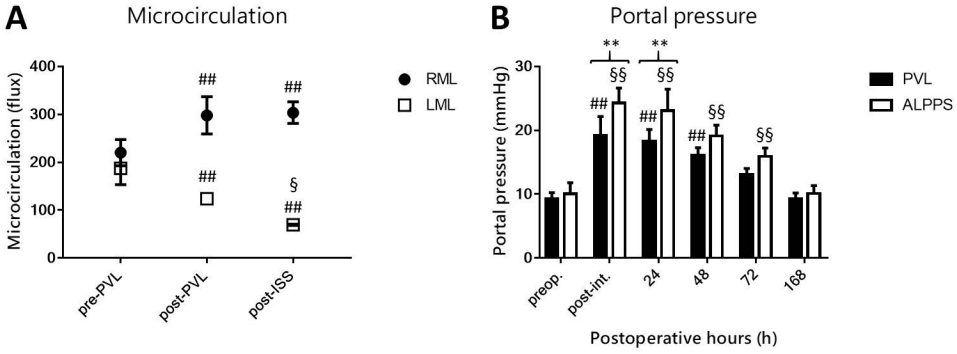

Figure 20. Effect of portal vein ligation (PVL) and associating liver partition and portal vein ligation for staged hepatectomy (ALPPS) on the liver microcirculation and portal pressure. The microcirculatory flow measurements (**A**) were performed preoperatively (pre-PVL), after PVL (post-PVL), and after the in-situ split in ALPPS (post-ISS) in the non-ligated right median lobe (RML) and the ligated left median lobe (LML) (n = 6 per time point per group). ## $p < 0.001$ versus preoperative value (pre-PVL); § $p < 0.05$, §§ $p < 0.001$ versus post-PVL value (post-PVL). The portal pressure measurements (**B**) were performed preoperatively (preop.), immediately after intervention (post-int.) and at 24 h, 48 h, 72 h, and 168 h after PVL and ALPPS (n = 6 per time point per group). ** $p < 0.001$ versus PVL; ## $p < 0.001$ PVL versus corresponding controls (preop.); § $p < 0.05$, §§ $p < 0.001$ ALPPS versus corresponding controls (preop.). Statistical analysis was performed with a two-way ANOVA and Tukey's post hoc test. Data are presented as mean ± 1 standard deviation (SD). Figure was adapted without modifications from: Daradics N. et al: Curr Oncol 2021.

4.3.4. Both systemic and portal BA concentrations increase following ALPPS

"PVL and the ALPPS resulted in a spike in systemic BA concentration from 24 h to 72 h after the intervention, which normalized to baseline levels at 168 h (Figure 21A). Systemic BA concentration was higher in the ALPPS group compared to the PVL group from 24 h

to 72 h. BA levels in the portal circulation did not change in the PVL group but became elevated from 48 h to 168 h following ALPPS, which resulted in a disparity between the groups from 48 h to 72 h (Figure 21B). (87)*"*

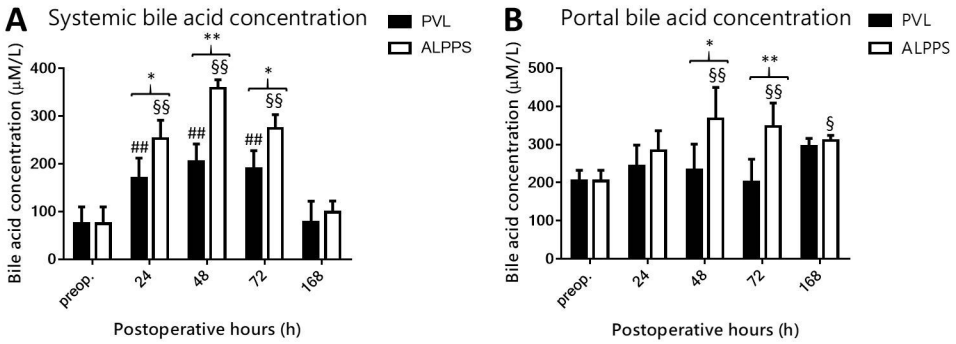

Figure 21. Effect of portal vein ligation (PVL) and associating liver partition and portal vein ligation for staged hepatectomy (ALPPS) on systemic bile acid (BA) concentration (A) and portal BA concentration (B). BA levels were determined preoperatively (preop.) and at 24 h, 48 h, 72 h, and 168 h after PVL and ALPPS (n = 6 per time point per group). * $p < 0.05$, ** $p < 0.001$ versus PVL; ## $p < 0.001$ PVL versus corresponding controls (preop.); § $p < 0.05$, §§ $p < 0.001$ ALPPS versus corresponding controls (preop.). Statistical analysis was performed with a two-way ANOVA and Tukey's post hoc test. Data are presented as mean ± 1 standard deviation (SD). Figure was adapted without modifications from: Daradics N. et al: Curr Oncol 2021.

4.3.5. Alterations in the expression of BA transporters and production enzymes following ALPPS

*"Following PVL, hepatocytes in the right median lobe reduced the expression of the BA importer sodium taurocholate co-transporting polypeptide (Ntcp) in the overall basolateral transport cascade, with no changes in organic anion transporting polypeptide (Oatp)1a4 and multidrug resistance protein (Mrp)3*levels *(22A–C). ALPPS, in contrast, accounted for a reduction* in *Oatp1a4 (at 24 h post-intervention; Figure 22A) and sodium/taurocholate cotransporting polypeptide* (*Ntcp) (at 48 h and 72 h post-intervention; Figure 22B), which suggests an attempt towards reaching BA homeostasis following a surge in BA influx. This is supported by the increase in transcript levels of the basolateral exporter Mrp3 at 72 h post-ALPPS (Figure 22C). Neither intervention had a notable effect on canalicular export of BAs via* Mrp2 *or bile salt exporting pump*

(Bsep) (Figure 22D-E, respectively) or BA synthesis, as reflected by the unchanged expression levels of cytochrome P450 isoform 7A1 (Cyp7a1) (Figure 22F). (87)*"*

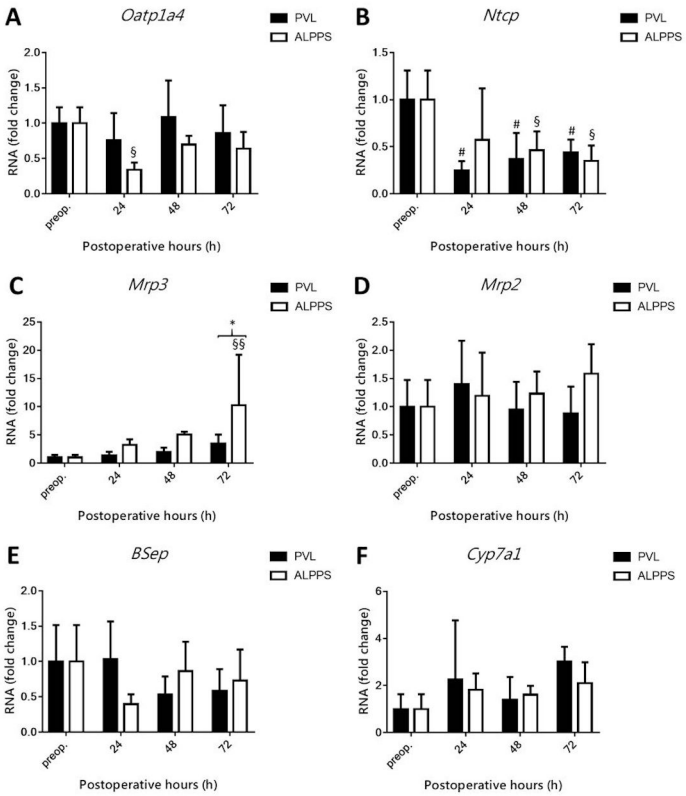

Figure 22. Effect of portal vein ligation (PVL) and associating liver partition and portal vein ligation for staged hepatectomy (ALPPS) on mRNA levels of hepatic bile acid production enzymes and transporters. Transcript levels of Oatp1a4 (**A**), Ntcp (**B**), Mrp3 (**C**), Mrp2 (**D**), Bsep (**E**), and Cyp7a1 (**F**) were determined preoperatively (preop.) and at 24 h, 48 h, 72 h, and 168 h after PVL and ALPPS (n = 6 per time point per group). * $p < 0.05$, # $p < 0.05$ PVL versus corresponding controls (preop.); § $p < 0.05$, §§ $p < 0.001$ ALPPS versus corresponding controls (preop.). Statistical analysis was performed with a two-way ANOVA and Tukey's post hoc test. Data are presented as mean ± 1 standard deviation (SD). Figure was adapted without modifications from: Daradics N. et al: Curr Oncol 2021.

4.3.6. Hepatic Fxr signaling is downmodulated both after PVL and ALPPS

"As presented in 23A, hepatic Fxr levels decreased after PVL in the hypertrophy response phase (72 h to 168 h). ALPPS also caused a decline in Fxr levels, but earlier than 24 h, and remained lower relative to preoperative levels up to 168 h after the

intervention. No intergroup differences were observed at any of the time points. Forkhead box (Fox)m1b, the downstream target of Fxr, exhibited a similar trend to Fxr in the PVL-exposed animals in that its transcript levels were decreased compared to baseline (23B). In the ALPPS group Foxm1b levels were also lower relative to preoperative levels at all time points, altogether suggesting anti-mitogenic signaling in this pathway, which is in contrast to the liver growth data in Figure 1. Shp did not seem to interfere in BA signaling following PVL and ALPPS given the absence of dysregulation (23C). (87)*"*

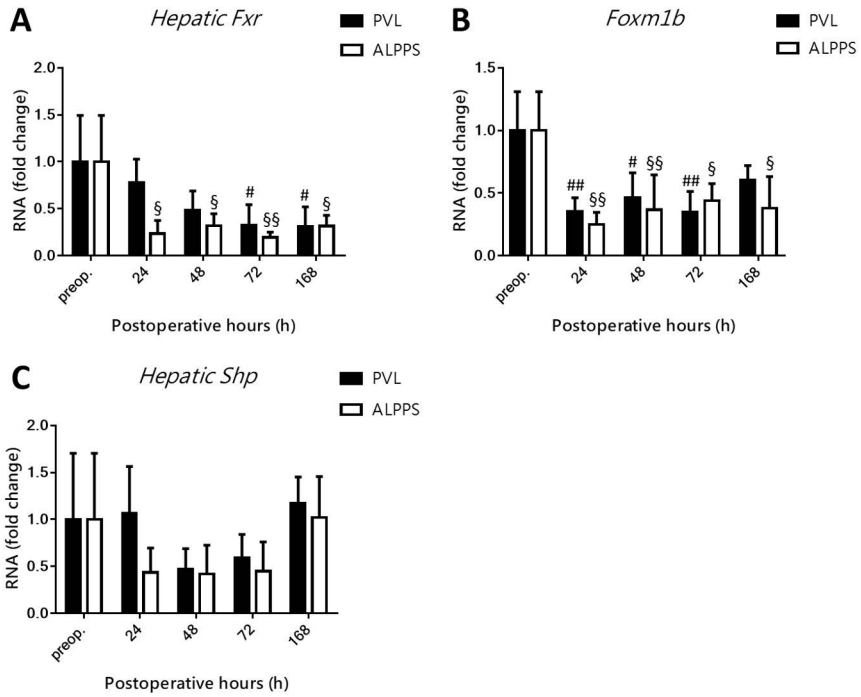

Figure 23. Effect of portal vein ligation (PVL) and associating liver partition and portal vein ligation for staged hepatectomy (ALPPS) on the hepatic Fxr pathway. Hepatic Fxr (A), Shp (B), and Foxm1b (C) transcript levels were determined preoperatively (preop.) and at 24 h, 48 h, 72 h, and 168 h after PVL and ALPPS (n = 6 per time point per group). # $p < 0.05$, ## $p < 0.001$ PVL versus corre-sponding controls (preop.); § $p < 0.05$, §§ $p < 0.001$ ALPPS versus corresponding controls (preop.). Statistical analysis was performed with a two-way ANOVA and Tukey's post hoc test. Data are presented as mean ± 1 standard deviation (SD). Figure was adapted without modifications from: Daradics N. et al: Curr Oncol 2021.

4.3.7. Upregulation of the ileal Fxr pathway after ALPPS

"Ileal Fxr showed no change after PVL but exhibited a spike at 24 h after ALPPS, while remaining at similar levels to baseline at all other time points in both groups (24A). This resulted in a notable difference between ALPPS and PVL at 24 h. Concomitantly, Shp had remained unchanged in the PVL group, while its upregulation was observed in the ileum of ALPPS-subjected animals at 24 h post-intervention, which had receded to baseline levels at the subsequent time point (Figure 24B). Ileal Fgf15 coincidentally did not change in the PVL group. A single time point spike was observed after ALPPS at 24 h (Figure 24C). Upregulation of Fgfr4 was not observed after PVL. ALPPS-exposed hepatocytes had upregulated Fgfr4 at 24 h, 48 h, and 168 h (Figure 24D), the protein product of which constitutes the cognate receptor for ileal Fgf15. (87)

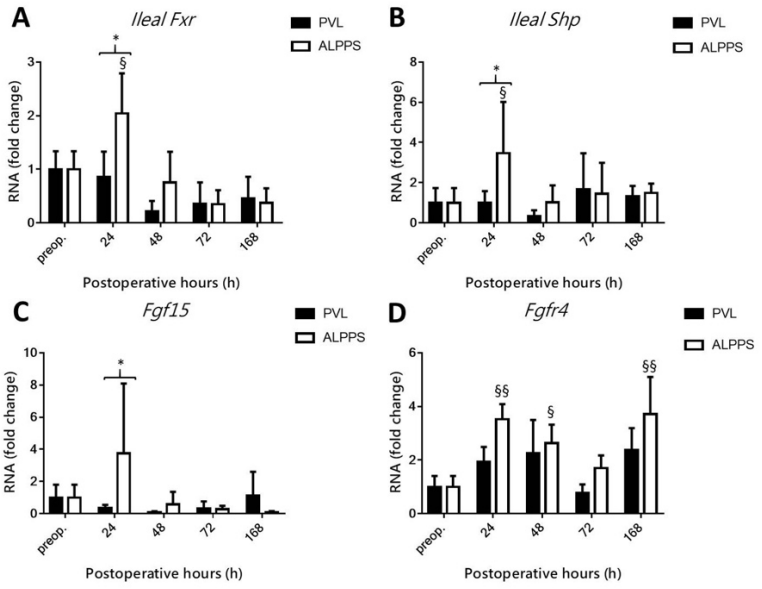

Figure 24. Effect of portal vein ligation (PVL) and associating liver partition and portal vein ligation for staged hepatectomy (ALPPS) on the intestinal Fxr pathway. Intestinal Fxr (**A**), intestinal Shp (**B**), Fgf15 (**C**), and Fgfr4 (**D**) were determined preoperatively (preop.) and at 24 h, 48 h, 72 h, and 168 h after PVL and ALPPS (n = 6 per time point per group). * $p < 0.05$; § $p < 0.05$, §§ $p < 0.001$ ALPPS versus corresponding controls (preop.). Statistical analysis was performed with a two-way ANOVA and Tukey's post hoc test. Data are presented as mean ± 1 standard deviation (SD). Figure was adapted without modifications from: Daradics N. et al: Curr Oncol 2021.

DOI:10.14753/SE.2023.2809

5. Discussion

"ALPPS is an emerging surgical intervention offered to select patients with liver tumors that are inoperable by standard techniques. As with PVL, which comprises an integral part of ALPPS, the main aim is to amplify the rate of liver regeneration in the FLR in order to enable safe resection of the tumor-containing liver lobes (87)*."*

Although ALPPS has numerous advantages, high postoperative mortality and morbidity provoked intense debate regarding its safety (48). In light of the unfavorable sides of ALPPS, its potential advantages could only be considered beneficial over standard techniques if the mortality and morbidity rates indicating the postoperative outcome is reduced to a level comparable to the standard procedures.

To diminish the postoperative complications, a novel concept has been raised in oncological surgery, called prehabilitation (7). One essential pillar of prehabilitation is PP, which enhances the patients' bearing capacity by preoperative exercise therapy. Although it has been extensively investigated in colorectal surgery (55), the effects of PP in liver surgery are still less known (57,60,100,101). As demonstrated in our previous investigation, PP could stabilize mitochondrial function following ALPPS (71), however to our knowledge there is no literature data on the effect of PP on the liver function and surgical complications after ALPPS.

Therefore, in our I. experiment we aimed to investigate whether the improvement of the cell-energy state is also translated into the improvement of the postoperative outcome of ALPPS. Remarkably, our main findings show that PP enhanced not only [1] liver regeneration, [2] but also improved postoperative liver function and [3] reduced postoperative vulnerability.

In accordance with our previous study (71), our results show that PP boosted further the inherently robust liver growth after ALPPS, increasing liver mass by more than 60% in the PP group compared to the S animals. Corroboratively, both cell proliferation in the FLR and the FLRV assessed by MRI were significantly higher in the PP group.

As already mentioned, the functional regeneration of the FLR in many cases could not keep pace with the prompt volumetric regeneration after ALPPS, subsequentially generating immature hepatocytes (50,102). We have previously demonstrated that after ALPPS, underdeveloped and malfunctioning mitochondria could be detected in the hepatocytes appertaining to the FLR (51). In our subsequent study we utilized PP to enhance the function and biogenesis of the mitochondria after ALPPS (71). Therefore, we hypothesized that PP also has a considerable effect on the functional regeneration of the FLR. Bilirubin and liver transaminases remained close to the normal level in the PP group, while they significantly increased in the S animals at 24 h also corroborating with previous investigations (103). Although the changes in laboratory parameters support our hypothesis, they could not be accounted as sufficient results, being informative only on whole liver function. Hence, to confirm our hypothesis we have selectively investigated the function of the FLR along with distinguishing the uptake and excretion of the regenerating liver by utilizing ^{99m}Tc-mebrofenin HBS, which has been described as an adequate and highly relevant method to measure the function of the FLR after two-stage hepatectomies, including ALPPS (37,50). Corroborating with static liver function tests, the dynamic functional measurement of the liver by ^{99m}Tc-mebrofenin HBS indicated enhanced FLR function in the PP group compared to the S group. A functional improvement could be observed on the excretory side, while intriguingly the uptake function of the two groups was similar. The altered function of MRP2, which is responsible for the excretion of ^{99m}Tc-mebrofenin (104), could contribute to the improvement of the hepatic excretory function, as its upregulation in the upper gastrointestinal system was documented after PP (105). This phenomenon is also echoed in our study, however further validation of the transcriptome on a molecular level is needed in the future.

While previous studies described the effects of prehabilitation only after hepatectomy (57,58,60,100), in our experiment we have demonstrated for the first time the favorable effect of PP on both whole and regional liver function after ALPPS.

As hepatic functional regeneration notably changes in the first 24–48 hours after ALPPS, which is the most vulnerable period following two-stage hepatectomies (106), we were eager to investigate whether PP could also affect the vulnerability following ALPPS.

After setting up an LPS-induced endotoxemia model, striking difference manifested in the postoperative mortality of the two groups, as more than 90 percent of animals survived in the PP group, while survival was only 41 percent in the S group indicating a decreased postoperative vulnerability after PP. In accordance with mortality rates, sepsis-related laboratory parameters such as CRP, thrombocytopenia, neutrophilia and lymphocytopenia also showed ameliorated values in the PP group. To our knowledge, this is the first description of the beneficial effect of PP on postoperative vulnerability.

On account of the novelty of our experiment, the validation of the utilized PP model was inevitable, hence the results were benchmarked against relevant literature data.
Preoperative MRI studies show that visceral and subcutaneous fat significantly decreased after PP in our model, yielding the same results as previous reports (107,108). As with changes in muscle volume, no difference could be detected between the two groups, which is also in accordance with investigations utilizing aerobic exercise modality (107–109). Aerobic training, for example with treadmill running, has a notable beneficial effect on body composition by decreasing body fat, however it does have an impact on muscle growth, which could be developed only with resistance training (109).

Given the fact that our PP model improved body fat composition, one pressing question remained to be answered: “is there a correlation between volumetric or functional regeneration and body fat composition?” To address this last question, univariable linear regression analysis was performed on our data, which evidenced an early supportive effect of decreased subcutaneous fat in liver volumetric regrowth. To our best knowledge, this is the first demonstration of the correlation between liver regeneration and body composition in the early and most vulnerable phase of liver regeneration after ALPPS.

Therefore, the I. experiment demonstrated the beneficial effect of PP after ALPPS, as not only the volumetric but also the functional regeneration of the liver improved along with enhanced stress-tolerance after surgery. Therefore, we propose the further clinical investigation of preoperative aerobic physical exercise protocols to improve patients’ safety after surgery.

In case of elderly, weakened patients preoperative conditioning could be proven crucial however, its feasibility is of course compromised. A solution to this problem could be the identification of the molecular targets in liver regeneration after ALPPS, which could create the ground of "pharmacological prehabilitation" and hence similar effects to the ones of PP could be achieved in case of frail patients, who could not tolerate extra physical burden. Therefore, we have continued our investigation to find novel possibilities of "pharmacological prehabilitation".

As previously shown in our study, a key component of the delayed functional recovery of the hepatocytes after ALPPS might be the energy disbalance caused by the insufficiency of mitochondria (51). Therefore, in the II. experiment, we hypothesized that the disadvantageous aspects of ALPPS could be also countered with mitochondrial therapy. In the pathophysiological conditions of the liver CypD inhibition has been already described as an effective mitochondrial therapy (72), therefore we aimed to investigate its effect on the mitochondrial dysfunction following ALPPS.

Utilizing a CypD KO mice model striking changes manifested in the cell-energy supply of the hepatocytes appertaining to the FLR after ALPPS. We identified in the CypD KO group (1) improved mitochondrial function; (2) enhanced mitochondrial biogenesis (3) delayed activation of caspase-3 and (4) accelerated liver growth.

In the course of liver regeneration cell division necessitates extensive energy supply after hepatectomy (75) and particularly in the robust liver regrowth following ALPPS (47). In contrast to the high energy demand of ALPPS, our previous study identified impaired mitochondrial function and biogenesis (51), which further increases the discrepancy between the energy demand and supply of the hepatocytes, possibly contributing to the high mortality and morbidity rates following ALPPS. Corroborating with our previous study (51), mitochondrial function was damaged in the WT group with decreased oxygen consumption and ATP production after ALPPS.

CypD provides enhanced permeability of the inner membrane of the mitochondria and subsequentially the dissipation of the mitochondrial membrane potential and interruption of ATP production (110). We hypothesized that its depletion could improve

mitochondrial function following ALPPS. In compliance with this, in the CypD KO mice both oxygen consumption and ATP production displayed higher levels, indicating higher and retained mitochondrial function. These results are also in accordance with literature data reporting the effect of CypD inhibition on mitochondrial function and cell energy supply (73,80,111).

To further analyze the cell energy production, investigation of the intramitochondrial NAD(P)H content was performed. Corroborating with our previous study (51), the level of intramitochondrial NAD(P)H decreased in the WT mice following ALPPS. The CypD KO group displayed similarly reduced NAD(P)H content indicating that CypD depletion effects only the terminal oxidation. As oxidative phosphorylation is the primary energy source of proliferating hepatocytes (75), this result does not contradict the effectiveness of CypD inhibition, but provides a deeper insight into its mechanism.

In our previous investigations we have also documented that mitochondrial biogenesis and protein production is deteriorated following ALPPS due to a prolonged and overwhelming inflammatory response (51,71), as TNF-α reduces the level of PGC1-α via nuclear factor kappa-light-chain-enhancer of activated B cells (NF-κB). Supporting this, PGC1-α level was strongly supressed in the WT group after ALPPS.
Relevant literature describes attenuated TNF-α and NF-κB levels as the effect of CypD depletion (112), hence we hypothesized that it also counters an impact on the PGC1-α regulated mitochondrial biogenesis pathway after ALPPS. The increased level of PGC1-α manifesting in the CypD KO mice compared both to the WT and the preoperative state groups verified our assumption. Although these changes did not translate into the increase of NRF1, which is a transcriptional factor of mitochondrial respiratory complexes (113), the I-II. protein complexes of the OXPHOS increased in the CypD KO group indicating the improvement not only in the function of the oxidative phosphorylation but also the enhanced biogenesis of its proteins. While it has been suggested by previous reports that CypD regulates the OXPHOS system by various kinds of mechanisms (114), to our knowledge this is the first demonstration that CypD depletion has an impact on the translation of the OXPHOS system.

CypD could induce cell death via the opening of the mPTP on two major routes. Firstly, the mPTP opening leads to the depolarization of the inner mitochondrial membrane resulting in the failure of the oxidative phosphorylation and consequently the necrosis of the cell (115). Secondly, opened mPTP also causes the swelling of the mitochondria, which engenders the rupture of the mitochondria and inevitably the release of cytochrome c from the inner space, which activates the apoptotic cascade via caspases and through the inhibition of PARP activity (72,116).

While investigating whether CypD depletion also impacts mitochondrial apoptosis, we have registered striking changes. Delayed activation of caspase-3 took shape in the CypD KO group, as its level only raised from 72 h to 168 h. On the contrary, activated caspase-3 level elevated already at 24 h in the WT group. The two phases of liver regeneration after ALPPS could serve as explanation to this phenomenon. In the initial phase of regeneration (which has been described as the most vulnerable phase lasting until 48th postoperative hour) portal pressure and microcirculation increases consequently activating cytokines and the regeneration cascade. In the second, remodelling phase from 72 h to 168 h apoptotic cell death creates the opportunity for the elimination of the redundant hepatocytes together with the reconstruction of hepatic cords (43). There is no doubt that further investigations are needed regarding the effect of CypD inhibition on the exact patomechanism of apoptosis, however our findings draw attention to the possibility that CypD depletion could also have a beneficial impact on apoptosis following ALPPS.

Numerous investigations indicated a correlation between mitochondrial activity and liver regeneration. After partial hepatectomy the buffered mitochondrial Ca^{2+} induced liver regeneration via the inhibition of apoptosis and with an additional direct effect on cell proliferation controlled by the shift in B-cell lymphoma protein 2 (Bcl-2)-associated X (Bax)/Bcl-2 (117), while after quarter-size liver transplantation liver regeneration could be augmented with a CypD inhibitor (NIM811) (80). Considering these reports, we were eager to investigate the effect of CypD depletion on liver regrowth after ALPPS. Our results supported the data in literature, as liver growth increased in the CypD KO group compared to the WT mice. Regarding cell proliferation no difference could be detected

between the groups, suggesting that CypD depletion does not directly affect regeneration, rather exerts its effect through the modulation of apoptosis.
Based on our results, mitochondrial therapy by CypD inhibition could be exploited in clinical studies as an effective pharmacological prehabilitation to mitigate the adverse events of ALPPS.

Aiming to provide various potential therapeutic possibilities for ALPPS, we further investigated molecular targets, which could be utilized as pharmacological prehabilitation. Therefore, we investigated in the III. experiment the role of BAs and the comprehensive Fxr signaling axis (hepatic and ileal) in the context of liver regeneration following PVL and ALPPS (87). Although previous reports have described earlier the importance of the primary nuclear BA receptor Fxr in liver regeneration (82,118), at the time of investigation no literature data were available regarding ALPPS.

By creating an experimental model, we found in the III. experiment that (1) the liver regrowth in the FLR was more explicit after ALPPS than PVL, (2) BA concentration both in systemic and portal circulation were notably higher after ALPPS than PVL, (3) although BA concentrations were profoundly elevated, they did not activate the hepatic Fxr signaling following either intervention, and (4) ALPPS but not PVL induced transcriptional upregulation of the ileal Fxr signaling. These findings partly contradict our hypothesis regarding BA-induced hepatic Fxr-mediated hepatocellular proliferation but confirm the ileal Fxr signaling aspects (87).

As our results in certain extent contrast the reported findings of BA-mediated liver regeneration following hepatectomy (81), the validation of the currently utilized animal model was necessary to exclude the possibility that the deviating findings from the putative framework engendered from technical elements rather than physiological and biochemical phenomena. Therefore, relevant results were benchmarked against literature data.

The growth of the FLR was more extensive after ALPPS than PVL, which corroborates with the experimental and clinical reports (119–122). Supporting this, cell division

measured with ki67 index was also notably higher in the ALPPS group compared to PVL, proving that liver growth did not engender from cellular swelling but from efficient hepatocyte proliferation, which is also in accordance with previous findings (5).

It is well-known that both PVL and ALPPS have a considerable impact on the liver circulation (43,45). Following the procedure, microcirculation of the ligated lobes transiently decreases (43,121), while portal pressure parallelly increases as the venous blood flow of the splanchnic circulation is forced to pass through a decreased vascular diameter (123,124). Our model yielded the same results, as microvascular circulation measured with laser Doppler-flowmeter was notably impaired in the ligated lobe in both interventions, but more prominently after ALPPS, which may be attributed to the transection disrupting the collateral circulation between the FLR and the ligated lobes (125). Adding to this, portal pressure was also significantly higher in both groups, further validating our model, however in case of ALPPS again higher values were detected.

Striking literature reports were published regarding the linkage between portal hypertension and intestinal permeability (126), which activates FXR signaling, and it is even more prominent in case of liver injury (127), hence more pertinent to ALPPS than PVL. Our findings are therefore supported by literature, as ileal Fxr showed no upregulation after PVL, while a significant increase was observed after ALPPS.

Numerous previous studies report prompt increase of BA plasma levels after hepatectomy due to the reduced uptake capacity of the hepatic tissue being responsible for BA plasma clearance (84,85,128,129). Additionally, canalicular networks in the FLR regenerate worse after ALPPS than in PVE, resulting in the leakage of the BAs into the circulation (130). As expected, elevation of plasma BA levels was observed after PVL and ALPPS in our model, whereby ALPPS resulted in higher BA levels than PVL (87).

The correspondence between our results and literature data hence exclude the probability that technical flaws accounted for the deviation of our data from literature results.

Given the evidence that our model is accurately utilized, we aimed to investigate why BA-derived hepatic Fxr mitogenic signals have no effect on the FLR after ALPPS. It has been evidenced that hepatic transporters are expressed to protect the hepatocyte by balancing the BA influx and composition of the cell after liver-reducing procedures such as hepatectomy (91,131–133). Hepatectomy, being a volume-restrictive intervention, also

activates hepatic Fxr signaling (91,131), which was however obviously downregulated in our model both after PVL and ALPPS. As we detected increased BA concentration both in the systemic and portal circulation, we were eager to investigate whether hepatocytes contributed to the increased BA load after PVL and ALPPS. The influx of BA is carried out by OATPs and NTCP at the basolateral end, while it is exported
basolaterally by MRP3 and 4 as well as OSTα and β, and at the canalicular end MRP2, BSEP and multidrug resistance associated protein (MDR)2 into the biliary tract. Mediated by CYP7A1, hepatocytes could also produce BA from cholesterol (81).
Although no proteomic analysis was performed, based on our transcriptome analysis we believe that hepatocytes further contributed to the BA overload by downregulating transcript levels of both basolateral importers and by increasing mRNA expression of the basolateral exporter Mrp3, which is regulated independently of Fxr and functions to protect hepatocytes from excessive exposure of toxic BAs (134,135). These findings suggest that hepatocytes endeavored to diminish toxic intracellular BA levels by basolaterally upregulating the transporters. This also might explain, why the hepatic Fxr pathway did not activate, Nevertheless, further speculations are futile without analyzing with molecular interventions the Fxr-Foxm1b pathway (87).

The last pressing question was whether in the ALPPS induced liver regeneration an additional BA signaling pathway was involved than the Fxr-Foxm1b pathway. Therefore, we investigated the intestinal Fxr pathway, which initiates liver regeneration through the ileum-derived Fgf15 that activates the Fgfr4 receptor on hepatocytes. Upon binding, Fgfr4 induce cell proliferation independently of Foxm1b via mitogen activated protein kinases (MAPK) and NF-κB (87). Although activation of the Stat3 pathway by Fgf15-Fgfr4 has been described after ALPPS (136–138), it had no effect in our model given the downregulation of *Foxm1b*, a downstream target of Stat3 (81,87). Alternatively, BAs can trigger mitosis via the nuclear receptor pregnane X receptor (PXR) while bypassing Stat3 and Foxm1b (81), which could be a plausible explanation for the ALPPS-related observations (87).
In the final analysis, the ALPPS-induced liver regeneration is likely mediated Fgf15/Fgfr4 signaling axis and not by hepatic Fxr, which elaborates a different signaling pattern after ALPPS compared to both PVL and hepatectomy.

The limitations of the study must be acknowledged. While the rat model of ALPPS diverges in some extent from clinical practice due to the size and lobular structure of the liver. Rats are a standard model species in liver surgery. Furthermore, we also carefully designed the ALPPS model to resemble the clinical technique. Via the ligation of the right lateral, left part of the median, left lateral, and caudate lobes leading to the portal vein, 80 percent of the portal vein flow of the liver was ligated and the transection was performed on the ischemic line of the right and left median lobe. Regarding the II. experiment, although significant physiological and molecular differences could occur between rodents and humans, the energy production, mitochondrial structure and biogenesis are extremely conserved in mammals (139), as well as the PPIF gene encoding CypD in vertebrates (140), therefore data gained from rodents could be appropriately translated to humans. In the III. experiment, the molecular analyses were performed at the transcriptional level, thus further analysis of the data is needed at the proteomic level.

DOI:10.14753/SE.2023.2809

6. Conclusions

Conclusions of the I. experiment:

I./1 Our study revealed the beneficial impact of PP on volumetric liver regeneration, as it could further augment the inherently robust regeneration after ALPPS.

I./2 Along with volumetric growth of the liver, PP also improved the functional regeneration after ALPPS.

I/3 Moreover, our study raised evidence that PP decreased the vulnerability following ALPPS, and hence significantly reduced the postoperative mortality.

I/4 The validity of our model was also confirmed, as PP notably improved the body fat composition of the animals.

I/5 Our study also revealed the correlation between reduced body fat composition and enhanced volumetric liver regeneration after ALPPS, strongly confirming the beneficial effect of PP.

Based on the findings of the I. experiment, the disadvantageous aspects of ALPPS could be mitigated with physical prehabilitation, therefore we propose the further clinical implementation of preoperative aerobic physical exercise protocols to improve patients' safety after surgery.

DOI:10.14753/SE.2023.2809

Conclusions of the II. experiment:

II./1 CypD depletion significantly enhanced mitochondrial function, as both ATP production and oxygen consumption improved after ALPPS.

II./2 Along with enhanced function, CypD depletion also enhanced mitochondrial biogenesis following ALPPS.

II./3 CypD depletion improved liver regrowth after ALPPS, possibly via the alteration of apoptosis.

The results of the II. experiment draw attention to the relevance of mitochondrial therapy after ALPPS. Therefore, we propose the further investigation of CypD inhibition as a potential target of “pharmacological prehabilitation” to enhance the post-operative outcomes following ALPPS.

DOI:10.14753/SE.2023.2809

Conclusions of the III. experiment:

III./1 Our model was adequately utilized, as liver growth induced by ALPPS was significantly greater compared to PVL.

III./2 Hemodynamical changes were more expressed after ALPPS compared to PVL, as microcirculation notably decreased in the ligated lobes while portal pressure parallelly increased in the FLR.

III./3 Both systemic and portal BA concentrations were significantly higher following ALPPS than PVL.

III./4 Nor the expression of BA production enzymes, nor BA transporters changed significantly with the exception of the Mrp3 basolateral transporter.

III./5 In the final analysis we exposed that BA-activated mitotic signals could be characterized by the activation of the intestinal Fxr pathway rather than hepatic Fxr signaling after ALPPS.

In conclusion, the findings of the III. experiment point to a different pattern of BA-induced liver regeneration following ALPPS. Based on these results, we propose that intestinal Fxr should be investigated as a potential therapeutic target of "pharmacological prehabilitation" to enhance post-operative outcomes following ALPPS, which can be achieved through mitogenic BA mimetics that have been cleared by regulatory agencies and are being clinically implemented for other indications.

DOI:10.14753/SE.2023.2809

7. Summary

Associating Liver Partition and Portal vein ligation for Staged hepatectomy (ALPPS) is an emerging surgical intervention promoting accelerated liver regeneration for patients with inoperable hepatic tumors by standard techniques. However, apart from the remarkable advantages, initially high morbidity and mortality rates undermined its benefits. As evidence raised that prehabilitation could improve postoperative complications, we investigated the effect of physical prehabilitation (PP) on the postoperative outcome of ALPPS. Furthermore, we also aimed to identify potential molecular targets, which could create the ground of "pharmacological prehabilitation" being in favor of frail patients, who could not tolerate extra physical burden.

Male Wistar rats underwent ALPPS (I. and III. experiment) and (PVL) (III. experiment). Male wild type (WT) BL6/jk and Cyclophilin D knockout (CypD KO) mice underwent ALPPS procedure (II. experiment). The following measurements were performed in the experiments. I.: liver weight, Ki67 index magnetic resonance imaging (MRI) liver-volumetry, liver laboratory parameters, 99mTc-mebrofenin hepatobiliary scintigraphy (HBS), mortality and septic parameters (in endotoxemia model). II.: mitochondrial function, and -proteomic analysis of factors involved in mitochondrial biogenesis, regeneration rate and mitotic activity. III.: regeneration rate, Ki67 index, liver hemodynamic changes, bile acid (BA) levels, transcription of hepatic and intestinal farnesoid X receptor (FXR) signaling pathway, BA transport, and BA production.

PP improved volumetric and functional liver regeneration, along with postoperative vulnerability after ALLPS. CypD deletion improved mitochondrial function and biogenesis and enhanced liver growth after ALPPS. Hepatic FXR signaling were comparable between ALPPS and PVL, while a more profound activation of the intestinal FXR pathway was observed 24 h after ALPPS compared to PVL.

Our study demonstrated for the first time the beneficial role of PP on the postoperative outcomes of ALPPS. We found two further molecular targets, which could be utilized in pharmacological prehabilitation to mitigate the vulnerability after ALPPS. Based on our results the inhibition of CypD could be a pertinent mitochondrial therapy, while the induction of intestinal FXR signaling cascades could further enhance postoperative outcomes following ALPPS.

8. References

1. Dixon M, Cruz J, Sarwani N, Gusani N. The Future Liver Remnant: Definition, Evaluation, and Management. Am Surg 2020;87:276–286. doi: 10.1177/0003134820951451.
2. Cieslak KP, Runge JH, Heger M, Stoker J, Bennink RJ, van Gulik TM. New Perspectives in the Assessment of Future Remnant Liver. Dig Surg 2014;31:255–268. doi: 10.1159/000364836.
3. de Graaf W, van Lienden KP, van den Esschert JW, Bennink RJ, van Gulik TM. Increase in future remnant liver function after preoperative portal vein embolization. Br J Surg. 2011;98:825–834. doi: 10.1002/bjs.7456. Cited: in: PMID: 21484773.
4. Eshmuminov D, Raptis DA, Linecker M, Wirsching A, Lesurtel M, Clavien P-A. Meta-analysis of associating liver partition with portal vein ligation and portal vein occlusion for two-stage hepatectomy. Br J Surg. 2016;103:1768–1782. doi: 10.1002/bjs.10290. Cited: in: PMID: 27633328.
5. Eshmuminov D, Tschuor C, Raptis DA, Boss A, Wurnig MC, Sergeant G, Schadde E, Clavien P-A. Rapid liver volume increase induced by associating liver partition with portal vein ligation for staged hepatectomy (ALPPS): Is it edema, steatosis, or true proliferation? Surgery. 2017;161:1549–1552. doi: 10.1016/j.surg.2017.01.005. Cited: in: : PMID: 28410744.
6. Raptis DA, Linecker M, Kambakamba P, Tschuor C, Müller PC, Hadjittofi C, Stavrou GA, Fard-Aghaie MH, Tun-Abraham M, Ardiles V, Malagó M, Campos RR, Oldhafer KJ, Hernandez-Alejandro R, de Santibañes E , Machado MA, Petrowsky H, Clavien PA. Defining Benchmark Outcomes for ALPPS. Ann Surg 2019;270:835—841. doi: 10.1097/sla.0000000000003539.
7. Silver JK, Baima J. Cancer Prehabilitation: An Opportunity to Decrease Treatment-Related Morbidity, Increase Cancer Treatment Options, and Improve Physical and Psychological Health Outcomes. Am J Phys Med Rehabil 2013;92.
8. Abbas S, Lam V, Hollands M. Ten-year survival after liver resection for colorectal metastases: systematic review and meta-analysis. ISRN Oncol

2011/06/22. 2011;2011:763245. doi: 10.5402/2011/763245. Cited: in: : PMID: 22091431.

9. Lin L, Yan L, Liu Y, Qu C, Ni J, Li H. The Burden and Trends of Primary Liver Cancer Caused by Specific Etiologies from 1990 to 2017 at the Global, Regional, National, Age, and Sex Level Results from the Global Burden of Disease Study 2017. Liver Cancer 2020;9:563–582. doi: 10.1159/000508568.
10. Liu H, Zhu S. Present status and future perspectives of preoperative portal vein embolization. Am J Surg. 2009;197:686–690. doi: 10.1016/j.amjsurg.2008.04.022. Cited: in: : PMID: 19249737.
11. Guglielmi A, Ruzzenente A, Conci S, Valdegamberi A, Iacono C. How much remnant is enough in liver resection? Dig Surg. 2012;29:6–17. doi: 10.1159/000335713. Cited: in: : PMID: 22441614.
12. Ray S, Mehta NN, Golhar A, Nundy S. Post hepatectomy liver failure - A comprehensive review of current concepts and controversies. Ann Med Surg (Lond) 2018;34:4–10. doi: 10.1016/j.amsu.2018.08.012. Cited: in: : PMID: 30181871.
13. Zheng Y, Yang H, He L, Mao Y, Zhang H, Zhao H, Du S, Xu Y, Chi T, Xu H, Lu X, Sang X, Zhong S. Reassessment of different criteria for diagnosing post-hepatectomy liver failure: a single-center study of 1683 hepatectomy. Oncotarget 2017;8:89269–89277. doi: 10.18632/oncotarget.19360. Cited: in: : PMID: 29179518.
14. Rahbari NN, Reissfelder C, Koch M, Elbers H, Striebel F, Büchler MW, Weitz J. The Predictive Value of Postoperative Clinical Risk Scores for Outcome After Hepatic Resection: A Validation Analysis in 807 Patients. Ann Surg Oncol. 2011;18:3640–3649. doi: 10.1245/s10434-011-1829-6.
15. Balzan S, Belghiti J, Farges O, Ogata S, Sauvanet A, Delefosse D, Durand F. The ???50-50 Criteria??? on Postoperative Day 5. Ann Surg. 2005;242:824–829. doi: 10.1097/01.sla.0000189131.90876.9e.
16. Mullen JT, Ribero D, Reddy SK, Donadon M, Zorzi D, Gautam S, Abdalla EK, Curley SA, Capussotti L, Clary BM, Vauthey JN. Hepatic Insufficiency and Mortality in 1,059 Noncirrhotic Patients Undergoing Major Hepatectomy. J Am Coll Surg. 2007;204:854–862. doi: 10.1016/j.jamcollsurg.2006.12.032.

17. Rahbari NN, Garden OJ, Padbury R, Brooke-Smith M, Crawford M, Adam R, Koch M, Makuuchi M, Dematteo RP, Christophi C, Banting S, Usatoff V, Nagino M, Maddern G, Hugh TJ, Vauthey JN, Greig P, Rees M, Yokoyama Y, Fan S, Nimura Y, Figueras J, Capussotti L, Büchler MW, Weitz J. Posthepatectomy liver failure: A definition and grading by the International Study Group of Liver Surgery (ISGLS). Surgery. 2011;149:713–724. doi: 10.1016/j.surg.2010.10.001.
18. Ethun CG, Maithel SK. Determination of Resectability. Surgical Clinics of North America. 2016;96:163–181. doi: https://doi.org/10.1016/j.suc.2015.12.002.
19. Abdalla EK, Denys A, Chevalier P, Nemr RA, Vauthey J-N. Total and segmental liver volume variations: Implications for liver surgery. Surgery 2004;135:404–410. doi: https://doi.org/10.1016/j.surg.2003.08.024.
20. Johnson TN, Tucker GT, Tanner MS, Rostami-Hodjegan A. Changes in liver volume from birth to adulthood: A meta-analysis. Liver Transplantation 2005;11:1481–1493. doi: https://doi.org/10.1002/lt.20519.
21. Vauthey J-N, Abdalla EK, Doherty DA, Gertsch P, Fenstermacher MJ, Loyer EM, Lerut J, Materne R, Wang X, Encarnacion A, Herron, D., Mathey, C., Ferrari, G., Charnsangavej, C., Do, K.-A. and Denys, A. Body surface area and body weight predict total liver volume in Western adults. Liver Transplantation 2002;8:233–240. doi: https://doi.org/10.1053/jlts.2002.31654.
22. Karlo C, Reiner CS, Stolzmann P, Breitenstein S, Marincek B, Weishaupt D, Frauenfelder T. CT- and MRI-based volumetry of resected liver specimen: Comparison to intraoperative volume and weight measurements and calculation of conversion factors. Eur J Radiol 2010;75:e107–e111. doi: 10.1016/j.ejrad.2009.09.005.
23. Schindl MJ, Redhead DN, Fearon KCH, Garden OJ, Wigmore SJ, (eLISTER) ELS and TERG. The value of residual liver volume as a predictor of hepatic dysfunction and infection after major liver resection. Gut 2005;54:289–296. doi: 10.1136/gut.2004.046524. Cited: in: : PMID: 15647196.
24. Hammond JS, Guha IN, Beckingham IJ, Lobo DN. Prediction, prevention and management of postresection liver failure. British Journal of Surgery 2011;98:1188–1200. doi: 10.1002/bjs.7630.

25. Teh SH, Nagorney DM, Stevens SR, Offord KP, Therneau TM, Plevak DJ, Talwalkar JA, Kim WR, Kamath PS. Risk Factors for Mortality After Surgery in Patients With Cirrhosis. Gastroenterology 2007;132:1261–1269. doi: 10.1053/j.gastro.2007.01.040.
26. Schroeder RA, Marroquin CE, Bute BP, Khuri S, Henderson WG, Kuo PC. Predictive indices of morbidity and mortality after liver resection. Ann Surg 2006;243:373–379. doi: 10.1097/01.sla.0000201483.95911.08. Cited: in: : PMID: 16495703.
27. Hoekstra LT, de Graaf W, Nibourg GAA, Heger M, Bennink RJ, Stieger B, van Gulik TM. Physiological and Biochemical Basis of Clinical Liver Function Tests: A Review. Ann Surg 2013;257.
28. Kamath PS, Kim WR. The model for end-stage liver disease (MELD). Hepatology. 2007;45:797–805. doi: https://doi.org/10.1002/hep.21563.
29. Teh SH, Christein J, Donohue J, Que F, Kendrick M, Farnell M, Cha S, Kamath P, Kim R, Nagorney DM. Hepatic Resection of Hepatocellular Carcinoma in Patients With Cirrhosis: Model of End-Stage Liver Disease (MELD) Score Predicts Perioperative Mortality. Journal of Gastrointestinal Surgery. 2005;9:1207–1215. doi: https://doi.org/10.1016/j.gassur.2005.09.008.
30. Pugh RNH, Murray-Lyon IM, Dawson JL, Pietroni MC, Williams R. Transection of the oesophagus for bleeding oesophageal varices. BJS (British Journal of Surgery). 1973;60:646–649. doi: https://doi.org/10.1002/bjs.1800600817.
31. Manizate F, Hiotis SP, Labow D, Roayaie S, Schwartz M. Liver functional reserve estimation: state of the art and relevance for local treatments. J Hepatobiliary Pancreat Sci. 2010;17:385–388. doi: https://doi.org/10.1007/s00534-009-0228-x.
32. Rassam F, Olthof PB, Bennink RJ, van Gulik TM. Current Modalities for the Assessment of Future Remnant Liver Function. Visc Med. 2017/11/30. 2017;33:442–448. doi: 10.1159/000480385. Cited: in: : PMID: 29344518.
33. de Gasperi A, Mazza E, Prosperi M. Indocyanine green kinetics to assess liver function: Ready for a clinical dynamic assessment in major liver surgery? World J Hepatol. 2016;8:355–367. doi: 10.4254/wjh.v8.i7.355. Cited: in: : PMID: 26981173.

34. de Graaf W, Bennink RJ, Heger M, Maas A, de Bruin K, van Gulik TM. Quantitative Assessment of Hepatic Function During Liver Regeneration in a Standardized Rat Model. Journal of Nuclear Medicine. 2011;52:294. doi: 10.2967/jnumed.110.078360.
35. Pastor CM, Müllhaupt B, Stieger B. The Role of Organic Anion Transporters in Diagnosing Liver Diseases by Magnetic Resonance Imaging. Drug Metabolism and Disposition. 2014;42:675. doi: 10.1124/dmd.113.055707.
36. Ghibellini G, Leslie EM, Pollack GM, Brouwer KLR. Use of tc-99m mebrofenin as a clinical probe to assess altered hepatobiliary transport: integration of in vitro, pharmacokinetic modeling, and simulation studies. Pharm Res. 2008/05/30. 2008;25:1851–1860. doi: 10.1007/s11095-008-9597-0. Cited: in: : PMID: 18509604.
37. Tomassini F, D'Asseler Y, Linecker M, Giglio MC, Castro-Benitez C, Truant S, Axelsson R, Olthof PB, Montalti R, Serenari M, Chapelle T, Lucidi V, Sparrelid E, Adam R, Van Gulik T, Pruvot FR, Clavien PA, Bruzzese D, Geboes K, Troisi RI. Hepatobiliary scintigraphy and kinetic growth rate predict liver failure after ALPPS: a multi-institutional study. HPB. 2020;22:1420–1428. doi: 10.1016/j.hpb.2020.01.010.
38. Dinant S, de Graaf W, Verwer BJ, Bennink RJ, van Lienden KP, Gouma DJ, van Vliet AK, van Gulik TM. Risk Assessment of Posthepatectomy Liver Failure Using Hepatobiliary Scintigraphy and CT Volumetry. Journal of Nuclear Medicine. 2007;48:685. doi: 10.2967/jnumed.106.038430.
39. Lee KC, Kinoshita H, Hirohashi K, Kubo S, Iwasa R. Extension of surgical indications for hepatocellular carcinoma by portal vein embolization. World J Surg. 1993;17:109–115. doi: 10.1007/BF01655721.
40. Azoulay D, Castaing D, Krissat J, Smail A, Hargreaves GM, Lemoine A, Emile JF, Bismuth H. Percutaneous portal vein embolization increases the feasibility and safety of major liver resection for hepatocellular carcinoma in injured liver. Ann Surg. 2000;232:665–672. doi: 10.1097/00000658-200011000-00008. Cited: in: : PMID: 11066138.
41. Palavecino M, Chun YS, Madoff DC, Zorzi D, Kishi Y, Kaseb AO, Curley SA, Abdalla EK, Vauthey J-N. Major hepatic resection for hepatocellular carcinoma

with or without portal vein embolization: Perioperative outcome and survival. Surgery. 2009;145:399–405. doi: 10.1016/j.surg.2008.10.009.

42. Narula N, Aloia TA. Portal vein embolization in extended liver resection. Langenbecks Arch Surg. 2017;402:727–735. doi: 10.1007/s00423-017-1591-8.
43. Szijártó A, Fülöp A. Triggered liver regeneration: from experimental model to clinical implications. Eur Surg Res. 2015;54:148–161. doi: 10.1159/000368961. Cited: in: : PMID: 25592812.
44. Lang S, Loss M, Schlitt H. „In-situ-Split"- (ISS) Leberresektion: Neue Aspekte zu Technik und Indikation. Zentralblatt für Chirurgie - Zeitschrift für Allgemeine, Viszeral-, Thorax- und Gefäßchirurgie. 2013;139:212–219. doi: 10.1055/s-0032-1328742.
45. de Santibañes E, Clavien P-A. Playing Play-Doh to prevent postoperative liver failure: the "ALPPS" approach. Ann Surg. United States; 2012. p. 415–417.
46. Torres OJM, Fernandes ESM, Herman P. ALPPS: past, present and future. Arq Bras Cir Dig. 2015;28:155–156. doi: 10.1590/S0102-67202015000300001. Cited: in: : PMID: 26537135.
47. de Santibañes M, Boccalatte L, de Santibañes E. A literature review of associating liver partition and portal vein ligation for staged hepatectomy (ALPPS): so far, so good. Updates Surg. 2017;69:9–19. doi: 10.1007/s13304-016-0401-0. Cited: in: : PMID: 27766595.
48. Schadde E, Ardiles V, Robles-Campos R, Malago M, Machado M, Hernandez-Alejandro R, Soubrane O, Schnitzbauer AA, Raptis D, Tschuor C, Petrowsky H, De Santibanes E, Clavien PA. Early Survival and Safety of ALPPS: First Report of the International ALPPS Registry. Ann Surg. 2014;260.
49. Stavrou GA, Donati M, Fard-Aghaie MH, Zeile M, Huber TM, Stang A, Oldhafer KJ. Did the International ALPPS Meeting 2015 Have an Impact on Daily Practice The Hamburg Barmbek Experience of 58 Cases. Visc Med. 2017;33:456–461. doi: 10.1159/000479476.
50. Olthof PB, Tomassini F, Huespe PE, Truant S, Pruvot F-R, Troisi RI, Castro C, Schadde E, Axelsson R, Sparrelid E, Bennink RJ, Adam R, van Gulik TM, de Santibanes E. Hepatobiliary scintigraphy to evaluate liver function in associating liver partition and portal vein ligation for staged hepatectomy: Liver volume

overestimates liver function. Surgery. 2017;162:775–783. doi: 10.1016/j.surg.2017.05.022. Cited: in: : PMID: 28732555.

51. Budai A, Horváth G, Tretter L, Radák Z, Koltai E, Bori Z, Torma F, Lukáts Á, Röhlich P, Szijártó A, Fülöp A. Mitochondrial function after associating liver partition and portal vein ligation for staged hepatectomy in an experimental model. Br J Surg. 2019;106:120–131. doi: 10.1002/bjs.10978. Cited: in: : PMID: 30259964.
52. Jain R, Gibson L, Coburn N. Prehabilitation for surgical oncology patients: empowering patient volition. Supportive Care in Cancer. 2018;26:3665–3667. doi: 10.1007/s00520-018-4300-4.
53. Li C, Carli F, Lee L, Charlebois P, Stein B, Liberman AS, Kaneva P, Augustin B, Wongyingsinn M, Gamsa A, Kim DJ, Vassiliou MC, Feldman LS. Impact of a trimodal prehabilitation program on functional recovery after colorectal cancer surgery: a pilot study. Surg Endosc. 2013;27:1072–1082. doi: 10.1007/s00464-012-2560-5.
54. Tan KY. Geriatric Surgery Service - Our Journey Piloting in Colorectal Surgery and Future Challenges. Ann Acad Med Singap. 2017;46:317–320. Cited: in: : PMID: 28920132.
55. Fulop A, Lakatos L, Susztak N, Szijarto A, Banky B. The effect of trimodal prehabilitation on the physical and psychological health of patients undergoing colorectal surgery: a randomised clinical trial. Anaesthesia. 2020; doi: 10.1111/anae.15215. Cited: in: : PMID: 32761611.
56. Barberan-Garcia A, Ubré M, Roca J, Lacy AM, Burgos F, Risco R, Momblán D, Balust J, Blanco I, Martínez-Pallí G. Personalised Prehabilitation in High-risk Patients Undergoing Elective Major Abdominal Surgery: A Randomized Blinded Controlled Trial. Ann Surg. 2018;267:50–56. doi: 10.1097/SLA.0000000000002293. Cited: in: : PMID: 28489682.
57. Lin F-P, Visina JM, Bloomer PM, Dunn MA, Josbeno DA, Zhang X, Clemente-Sanchez A, Tevar AD, Hughes CB, Jakicic JM, Duarte-Rojo A. Prehabilitation-Driven Changes in Frailty Metrics Predict Mortality in Patients With Advanced Liver Disease. Official journal of the American College of Gastroenterology | ACG. 2021;116.

58. Dunne DFJ, Jack S, Jones RP, Jones L, Lythgoe DT, Malik HZ, Poston GJ, Palmer DH, Fenwick SW. Randomized clinical trial of prehabilitation before planned liver resection. Br J Surg. 2016;103:504–512. doi: 10.1002/bjs.10096. Cited: in: : PMID: 26864728.
59. Wang B, Shelat VG, Chow JJL, Huey TCW, Low JK, Woon WWL, Junnarkar SP. Prehabilitation Program Improves Outcomes of Patients Undergoing Elective Liver Resection. J Surg Res. 2020;251:119–125. doi: 10.1016/j.jss.2020.01.009. Cited: in: : PMID: 32135382.
60. Hao S, Reis HL, Wercholuk AN, Snyder RA, Parikh AA. Prehabilitation for Older Adults Undergoing Liver Resection: Getting Patients and Surgeons Up to Speed. J Am Med Dir Assoc. 2022; doi: 10.1016/j.jamda.2022.01.077.
61. Hao S, Reis HL, Quinn AW, Snyder RA, Parikh AA. Prehabilitation for Older Adults Undergoing Liver Resection: Getting Patients and Surgeons Up to Speed. J Am Med Dir Assoc. 2022;23:547–554. doi: 10.1016/j.jamda.2022.01.077.
62. Duarte-Rojo A, Ruiz-Margáin A, Montaño-Loza AJ, Macías-Rodríguez RU, Ferrando A, Kim WR. Exercise and physical activity for patients with end-stage liver disease: Improving functional status and sarcopenia while on the transplant waiting list. Liver Transplantation. 2018;24:122–139. doi: 10.1002/lt.24958.
63. Chou C-H, Hwang C-L, Wu Y-T. Effect of Exercise on Physical Function, Daily Living Activities, and Quality of Life in the Frail Older Adults: A Meta-Analysis. Arch Phys Med Rehabil. 2012;93:237–244. doi: 10.1016/j.apmr.2011.08.042.
64. Hulzebos EHJ, Smit Y, Helders PPJM, van Meeteren NLU. Preoperative physical therapy for elective cardiac surgery patients. Cochrane Database Syst Rev. 2012;11:CD010118–CD010118. doi: 10.1002/14651858.CD010118.pub2. Cited: in: : PMID: 23152283.
65. O'Doherty AF, West M, Jack S, Grocott MPW. Preoperative aerobic exercise training in elective intra-cavity surgery: a systematic review. Br J Anaesth. 2013;110:679–689. doi: 10.1093/bja/aes514.
66. Dronkers JJ, Chorus AMJ, van Meeteren NLU, Hopman-Rock M. The association of pre-operative physical fitness and physical activity with outcome after scheduled major abdominal surgery. Anaesthesia. 2013;68:67–73. doi: 10.1111/anae.12066.

67. Koelwyn GJ, Quail DF, Zhang X, White RM, Jones LW. Exercise-dependent regulation of the tumour microenvironment. Nat Rev Cancer. 2017;17:620–632. doi: 10.1038/nrc.2017.78.

68. Fiuza-Luces C, Santos-Lozano A, Joyner M, Carrera-Bastos P, Picazo O, Zugaza JL, Izquierdo M, Ruilope LM, Lucia A. Exercise benefits in cardiovascular disease: beyond attenuation of traditional risk factors. Nat Rev Cardiol. 2018;15:731–743. doi: 10.1038/s41569-018-0065-1.

69. Gleeson M, Bishop NC, Stensel DJ, Lindley MR, Mastana SS, Nimmo MA. The anti-inflammatory effects of exercise: mechanisms and implications for the prevention and treatment of disease. Nat Rev Immunol. 2011;11:607–615. doi: 10.1038/nri3041.

70. Zhang H, Chen T, Ren J, Xia Y, Onuma A, Wang Y, He J, Wu J, Wang H, Hamad A, Shen C, Zhang J, Asara JM, Behbehani GK, Wen H, Deng M, Tsung A, Huang H. Pre-operative exercise therapy triggers anti-inflammatory trained immunity of Kupffer cells through metabolic reprogramming. Nat Metab. 2021;3:843–858. doi: 10.1038/s42255-021-00402-x.

71. Fard-Aghaie MH, Budai A, Daradics N, Horvath G, Oldhafer KJ, Szijarto A, Fulop A. The effects of physical prehabilitation: Improved liver regeneration and mitochondrial function after ALPPS operation in a rodent model. J Hepatobiliary Pancreat Sci. 2021; doi: 10.1002/jhbp.945. Cited: in: : PMID: 33742528.

72. Naoumov N v. Cyclophilin inhibition as potential therapy for liver diseases. J Hepatol. 2014;61:1166–1174. doi: 10.1016/j.jhep.2014.07.008. Cited: in: : PMID: 25048953.

73. Elrod JW, Molkentin JD. Physiologic functions of cyclophilin D and the mitochondrial permeability transition pore. Circ J. 2013;77:1111–1122. doi: 10.1253/circj.cj-13-0321. Cited: in: : PMID: 23538482.

74. Rasola A, Bernardi P. Mitochondrial permeability transition in Ca(2+)-dependent apoptosis and necrosis. Cell Calcium. 2011;50:222–233. doi: 10.1016/j.ceca.2011.04.007. Cited: in: : PMID: 21601280.

75. Fu D, Mitra K, Sengupta P, Jarnik M, Lippincott-Schwartz J, Arias IM. Coordinated elevation of mitochondrial oxidative phosphorylation and autophagy

help drive hepatocyte polarization. Proceedings of the National Academy of Sciences. 2013;110:7288–7293. doi: 10.1073/pnas.1304285110.

76. Yamanoi A, Nagasue N, Kohno H, Chang YC, Hayashi T, Nakamura T. Attenuation of ischemia-reperfusion injury of the liver in dogs by cyclosporine. A comparative study with allopurinol and methylprednisolone. Transplantation. 1991;52:27–30. doi: 10.1097/00007890-199107000-00005. Cited: in: : PMID: 1858150.
77. Hayashi T, Nagasue N, Kohno H, Chang YC, Nakamura T. Beneficial effect of cyclosporine pretreatment in canine liver ischemia. Enzymatic and electronmicroscopic studies. Transplantation. 1991;52:116–121. doi: 10.1097/00007890-199107000-00024. Cited: in: : PMID: 1907040.
78. Lim SY, Davidson SM, Hausenloy DJ, Yellon DM. Preconditioning and postconditioning: the essential role of the mitochondrial permeability transition pore. Cardiovasc Res. 2007;75:530–535. doi: 10.1016/j.cardiores.2007.04.022. Cited: in: : PMID: 17512507.
79. Lawitz E, Godofsky E, Rouzier R, Marbury T, Nguyen T, Ke J, Huang M, Praestgaard J, Serra D, Evans TG. Safety, pharmacokinetics, and antiviral activity of the cyclophilin inhibitor NIM811 alone or in combination with pegylated interferon in HCV-infected patients receiving 14 days of therapy. Antiviral Res. 2011;89:238–245. doi: 10.1016/j.antiviral.2011.01.003. Cited: in: : PMID: 21255610.
80. Zhong Z, Theruvath TP, Currin RT, Waldmeier PC, Lemasters JJ. NIM811, a mitochondrial permeability transition inhibitor, prevents mitochondrial depolarization in small-for-size rat liver grafts. Am J Transplant. 2007;7:1103–1111. doi: 10.1111/j.1600-6143.2007.01770.x. Cited: in: : PMID: 17456198.
81. de Haan L, van der Lely SJ, Warps A-LK, Hofsink Q, Olthof PB, de Keijzer MJ, Lionarons DA, Mendes-Dias L, Bruinsma BG, Uygun K, Jaeschke H, Farrell GC, Teoh N, van Golen RF, Li T, Heger M. Post-hepatectomy liver regeneration in the context of bile acid homeostasis and the gut-liver signaling axis. J Clin Transl Res. 2018;4:1–46. doi: 10.18053/jctres.04.201801.001. Cited: in: : PMID: 30761355.

82. Huang W, Ma K, Zhang J, Qatanani M, Cuvillier J, Liu J, Dong B, Huang X, Moore DD. Nuclear receptor-dependent bile acid signaling is required for normal liver regeneration. Science. 2006;312:233–236. doi: 10.1126/science.1121435. Cited: in: : PMID: 16614213.

83. Geier A, Trautwein C. Bile acids are “homeotrophic” sensors of the functional hepatic capacity and regulate adaptive growth during liver regeneration. Hepatology. 2007;45:251–253. doi: https://doi.org/10.1002/hep.21521.

84. Uriarte I, Fernandez-Barrena MG, Monte MJ, Latasa MU, Chang HCY, Carotti S, Vespasiani-Gentilucci U, Morini S, Vicente E, Concepcion AR, Medina JF, Marin JJ, Berasain C, Prieto J, Avila MA. Identification of fibroblast growth factor 15 as a novel mediator of liver regeneration and its application in the prevention of post-resection liver failure in mice. Gut. 2013;62:899–910. doi: 10.1136/gutjnl-2012-302945. Cited: in: : PMID: 23292666.

85. Péan N, Doignon I, Garcin I, Besnard A, Julien B, Liu B, Branchereau S, Spraul A, Guettier C, Humbert L, Schoonjans K, Rainteau D, Tordjmann T. The receptor TGR5 protects the liver from bile acid overload during liver regeneration in mice. Hepatology. 2013;58:1451–1460. doi: 10.1002/hep.26463. Cited: in: : PMID: 23686672.

86. Borude P, Edwards G, Walesky C, Li F, Ma X, Kong B, Guo GL, Apte U. Hepatocyte-specific deletion of farnesoid X receptor delays but does not inhibit liver regeneration after partial hepatectomy in mice. Hepatology. 2012;56:2344–2352. doi: 10.1002/hep.25918. Cited: in: : PMID: 22730081.

87. Daradics N, Olthof PB, Budai A, Heger M, van Gulik TM, Fulop A, Szijarto A. The Role of Farnesoid X Receptor in Accelerated Liver Regeneration in Rats Subjected to ALPPS. Curr Oncol. 2021;28:5240–5254. doi: 10.3390/curroncol28060438. Cited: in: : PMID: 34940077.

88. Zhang L, Wang Y-D, Chen W-D, Wang X, Lou G, Liu N, Lin M, Forman BM, Huang W. Promotion of liver regeneration/repair by farnesoid X receptor in both liver and intestine in mice. Hepatology. 2012;56:2336–2343. doi: 10.1002/hep.25905. Cited: in: : PMID: 22711662.

89. Kong B, Huang J, Zhu Y, Li G, Williams J, Shen S, Aleksunes LM, Richardson JR, Apte U, Rudnick DA, Guo GL. Fibroblast growth factor 15 deficiency

impairs liver regeneration in mice. Am J Physiol Gastrointest Liver Physiol. 2014;306:G893-902. doi: 10.1152/ajpgi.00337.2013. Cited: in: : PMID: 24699334.

90. Olthof PB, Huisman F, Schaap FG, van Lienden KP, Bennink RJ, van Golen RF, Heger M, Verheij J, Jansen PL, Olde Damink SW, van Gulik TM. Effect of obeticholic acid on liver regeneration following portal vein embolization in an experimental model. British Journal of Surgery. 2017;104:590–599. doi: 10.1002/bjs.10466.
91. van Golen RF, Olthof PB, Lionarons DA, Reiniers MJ, Alles LK, Uz Z, de Haan L, Ergin B, de Waart DR, Maas A, Verheij J, Jansen PL, Damink SWO, Schaap FG, van Gulik TM, Heger M. FXR agonist obeticholic acid induces liver growth but exacerbates biliary injury in rats with obstructive cholestasis. Sci Rep. 2018;8:16529. doi: 10.1038/s41598-018-33070-1. Cited: in: : PMID: 30409980.
92. Ren W, Chen G, Wang X, Zhang A, Li C, Lv W, Pan K, Dong J-H. Simultaneous bile duct and portal vein ligation induces faster atrophy/hypertrophy complex than portal vein ligation: role of bile acids. Sci Rep. 2015;5:8455. doi: 10.1038/srep08455. Cited: in: : PMID: 25678050.
93. Kilkenny C, Browne WJ, Cuthill IC, Emerson M, Altman DG. Improving bioscience research reporting: the ARRIVE guidelines for reporting animal research. PLoS Biol. 2010;8:e1000412. doi: 10.1371/journal.pbio.1000412. Cited: in: : PMID: 20613859.
94. Bankhead P, Loughrey MB, Fernández JA, Dombrowski Y, McArt DG, Dunne PD, McQuaid S, Gray RT, Murray LJ, Coleman HG, ames JA, Salto-Tellez M, Hamilton PW. QuPath: Open source software for digital pathology image analysis. Sci Rep. 2017;7:16878. doi: 10.1038/s41598-017-17204-5. Cited: in: : PMID: 29203879.
95. Daradics N, Horvath G, Tretter L, Paal A, Fulop A, Budai A, Szijarto A. The effect of Cyclophilin D depletion on liver regeneration following associating liver partition and portal vein ligation for staged hepatectomy. PLoS One. 2022;17:e0271606-.
96. Daradics N, Levay K, Horvath I, Kovacs N, Mathe D, Szigeti K, Szijarto A, Fulop A. Physical prehabilitation improves the postoperative outcome of

associating liver partition and portal vein ligation for staged hepatectomy in experimental model. Sci Rep. 2022;12:19441. doi: 10.1038/s41598-022-23744-2.

97. Sotocina SG, Sorge RE, Zaloum A, Tuttle AH, Martin LJ, Wieskopf JS, Mapplebeck JCS, Wei P, Zhan S, Zhang S, McDougall JJ, King OD, Mogil JS. The Rat Grimace Scale: A Partially Automated Method for Quantifying Pain in the Laboratory Rat via Facial Expressions. Mol Pain. 2011;7:1744-8069-7–55. doi: 10.1186/1744-8069-7-55.
98. Rosenthal RE, Hamud F, Fiskum G, Varghese PJ, Sharpe S. Cerebral Ischemia and Reperfusion: Prevention of Brain Mitochondrial Injury by Lidoflazine. Journal of Cerebral Blood Flow & Metabolism. 1987;7:752–758. doi: 10.1038/jcbfm.1987.130.
99. Schindelin J, Arganda-Carreras I, Frise E, Kaynig V, Longair M, Pietzsch T, Preibisch S, Rueden C, Saalfeld S, Schmid B, Tinevez JY, White DJ, Hartenstein V, Eliceiri K, Tomancak P, Cardona A. Fiji: an open-source platform for biological-image analysis. Nat Methods. 2012;9:676–682. doi: 10.1038/nmeth.2019. Cited: in: : PMID: 22743772.
100. Mylius CF, Krijnen WP, Takken T, Lips DJ, Eker H, van der Schans CP, Klaase JM. Objectively measured preoperative physical activity is associated with time to functional recovery after hepato-pancreato-biliary cancer surgery: a pilot study. Perioper Med (Lond). 2021;10:33. doi: 10.1186/s13741-021-00202-7. Cited: in: : PMID: 34602089.
101. Lin F-P, Visina JM, Bloomer PM, Dunn MA, Josbeno DA, Zhang X, Clemente-Sanchez A, Tevar AD, Hughes CB, Jakicic JM, Duarte-Rojo A. Prehabilitation-Driven Changes in Frailty Metrics Predict Mortality in Patients With Advanced Liver Disease. Official journal of the American College of Gastroenterology | ACG. 2021;116.
102. Matsuo K, Murakami T, Kawaguchi D, Hiroshima Y, Koda K, Yamazaki K, Ishida Y, Tanaka K. Histologic features after surgery associating liver partition and portal vein ligation for staged hepatectomy versus those after hepatectomy with portal vein embolization. Surgery. 2016;159:1289–1298. doi: 10.1016/j.surg.2015.12.004. Cited: in: : PMID: 26775576.

103. Uribe M, Uribe-Echevarría S, Mandiola C, Zapata MI, Riquelme F, Romanque P. Insight on ALPPS – Associating Liver Partition and Portal Vein Ligation for Staged Hepatectomy – mechanisms: activation of mTOR pathway. HPB. 2018;20:729–738. doi: https://doi.org/10.1016/j.hpb.2018.02.636.
104. Ghibellini G, Leslie EM, Pollack GM, Brouwer KLR. Use of tc-99m mebrofenin as a clinical probe to assess altered hepatobiliary transport: integration of in vitro, pharmacokinetic modeling, and simulation studies. Pharm Res. 2008/05/30. 2008;25:1851–1860. doi: 10.1007/s11095-008-9597-0. Cited: in: : PMID: 18509604.
105. Parry TL, Hayward R. Exercise training does not affect anthracycline antitumor efficacy while attenuating cardiac dysfunction. American Journal of Physiology-Regulatory, Integrative and Comparative Physiology. 2015;309:R675–R683. doi: 10.1152/ajpregu.00185.2015.
106. Kameoka N, Chijiiwa K, Kozaki N, Makino I, Naito T, Tanaka M. Hepatic Adenine Nucleotides and DNA Synthesis during the Regenerative and Atrophic Process of the Liver Lobes after Selective Portal Vein Ligation. European Surgical Research. 1996;28:212–221. doi: 10.1159/000129459.
107. Mohammadi HR, Khoshnam MS, Khoshnam E. Effects of Different Modes of Exercise Training on Body Composition and Risk Factors for Cardiovascular Disease in Middle-aged Men. Int J Prev Med. 2018;9:9. doi: 10.4103/ijpvm.IJPVM_209_16. Cited: in: : PMID: 29441186.
108. Donges CE, Duffield R. Effects of resistance or aerobic exercise training on total and regional body composition in sedentary overweight middle-aged adults. Applied Physiology, Nutrition, and Metabolism. 2012;37:499–509. doi: 10.1139/h2012-006.
109. Willis LH, Slentz CA, Bateman LA, Shields AT, Piner LW, Bales CW, Houmard JA, Kraus WE. Effects of aerobic and/or resistance training on body mass and fat mass in overweight or obese adults. J Appl Physiol (1985). 2012/09/27. 2012;113:1831–1837. doi: 10.1152/japplphysiol.01370.2011. Cited: in: : PMID: 23019316.

110. Rolfe DF, Brand MD. The physiological significance of mitochondrial proton leak in animal cells and tissues. Biosci Rep. 1997;17:9–16. doi: 10.1023/a:1027327015957. Cited: in: : PMID: 9171916.
111. Hansson MJ, Morota S, Chen L, Matsuyama N, Suzuki Y, Nakajima S, Tanoue T, Omi A, Shibasaki F, Shimazu M, Ikeda Y, Uchino H, Elmér E. Cyclophilin D-sensitive mitochondrial permeability transition in adult human brain and liver mitochondria. J Neurotrauma. 2011;28:143–153. doi: 10.1089/neu.2010.1613. Cited: in: : PMID: 21121808.
112. Veres B, Eros K, Antus C, Kalman N, Fonai F, Jakus PB, Boros E, Hegedus Z, Nagy I, Tretter L, Gallyas F Jr, Sumegi B. Cyclophilin D-dependent mitochondrial permeability transition amplifies inflammatory reprogramming in endotoxemia. FEBS Open Bio. 2021/02/13. 2021;11:684–704. doi: 10.1002/2211-5463.13091. Cited: in: : PMID: 33471430.
113. Evans MJ, Scarpulla RC. NRF-1: a trans-activator of nuclear-encoded respiratory genes in animal cells. Genes Dev. 1990;4:1023–1034. doi: 10.1101/gad.4.6.1023. Cited: in: : PMID: 2166701.
114. Porter GAJ, Beutner G. Cyclophilin D, Somehow a Master Regulator of Mitochondrial Function. Biomolecules. 2018;8. doi: 10.3390/biom8040176. Cited: in: : PMID: 30558250.
115. Kim J-S, He L, Lemasters JJ. Mitochondrial permeability transition: a common pathway to necrosis and apoptosis. Biochem Biophys Res Commun. 2003;304:463–470. doi: 10.1016/s0006-291x(03)00618-1. Cited: in: : PMID: 12729580.
116. Schriewer JM, Peek CB, Bass J, Schumacker PT. ROS-mediated PARP activity undermines mitochondrial function after permeability transition pore opening during myocardial ischemia-reperfusion. J Am Heart Assoc. 2013;2:e000159–e000159. doi: 10.1161/JAHA.113.000159. Cited: in: : PMID: 23598272.
117. Guerra MT, Fonseca EA, Melo FM, Andrade VA, Aguiar CJ, Andrade LM, Pinheiro ACN, Casteluber MCF, Resende RR, Pinto MCX, Fernandes SO, Cardoso VN, Souza-Fagundes EM, Menezes GB, de Paula AM, Nathanson MH, Leite Mde F. Mitochondrial calcium regulates rat liver regeneration through the

modulation of apoptosis. Hepatology. 2011;54:296–306. doi: 10.1002/hep.24367. Cited: in: : PMID: 21503946.

118. Naugler WE. Bile acid flux is necessary for normal liver regeneration. PLoS One. 2014;9:e97426. doi: 10.1371/journal.pone.0097426. Cited: in: : PMID: 24841254.
119. Takamoto T, Sugawara Y, Hashimoto T, Makuuchi M. Associating liver partition and portal vein ligation (ALPPS): Taking a view of trails. Biosci Trends. 2015;9:280–283. doi: 10.5582/bst.2015.01131. Cited: in: : PMID: 26559019.
120. Shi JH, Hammarström C, Grzyb K, Line PD. Experimental evaluation of liver regeneration patterns and liver function following ALPPS. BJS Open. 2017;1:84–96. doi: 10.1002/bjs5.18. Cited: in: : PMID: 29951610.
121. Chan KS, Low JK, Shelat VG. Associated liver partition and portal vein ligation for staged hepatectomy: a review. Transl Gastroenterol Hepatol. 2020;5:37. doi: 10.21037/tgh.2019.12.01. Cited: in: : PMID: 32632388.
122. Glinka J, Ardiles V, Pekolj J, de Santibañes E, de Santibañes M. The role of associating liver partition and portal vein ligation for staged hepatectomy in the management of patients with colorectal liver metastasis. Hepatobiliary Surg Nutr. 2020;9:694–704. doi: 10.21037/hbsn.2019.08.03. Cited: in: : PMID: 33299825.
123. Lainas P, Boudechiche L, Osorio A, Coulomb A, Weber A, Pariente D, Franco D, Dagher I. Liver regeneration and recanalization time course following reversible portal vein embolization. J Hepatol. 2008;49:354–362. doi: 10.1016/j.jhep.2008.01.034. Cited: in: : PMID: 18387688.
124. Schoen JM, Wang HH, Minuk GY, Lautt WW. Shear stress-induced nitric oxide release triggers the liver regeneration cascade. Nitric Oxide. 2001;5:453–464. doi: 10.1006/niox.2001.0373. Cited: in: : PMID: 11587560.
125. Alvarez FA, Ardiles V, Sanchez Claria R, Pekolj J, de Santibañes E. Associating Liver Partition and Portal Vein Ligation for Staged Hepatectomy (ALPPS): Tips and Tricks. Journal of Gastrointestinal Surgery. 2013;17:814–821. doi: 10.1007/s11605-012-2092-2.
126. Simbrunner B, Mandorfer M, Trauner M, Reiberger T. Gut-liver axis signaling in portal hypertension. World J Gastroenterol. 2019;25:5897–5917. doi: 10.3748/wjg.v25.i39.5897. Cited: in: : PMID: 31660028.

127. Sorribas M, Jakob MO, Yilmaz B, Li H, Stutz D, Noser Y, de Gottardi A, Moghadamrad S, Hassan M, Albillos A, Francés R, Juanola O, Spadoni I, Rescigno M, Wiest R. FXR modulates the gut-vascular barrier by regulating the entry sites for bacterial translocation in experimental cirrhosis. J Hepatol. 2019;71:1126–1140. doi: 10.1016/j.jhep.2019.06.017. Cited: in: : PMID: 31295531.

128. Monte MJ, Martinez-Diez MC, El-Mir MY, Mendoza ME, Bravo P, Bachs O, Marin JJG. Changes in the pool of bile acids in hepatocyte nuclei during rat liver regeneration. J Hepatol. 2002;36:534–542. doi: 10.1016/s0168-8278(01)00296-3. Cited: in: : PMID: 11943426.

129. Doignon I, Julien B, Serrière-Lanneau V, Garcin I, Alonso G, Nicou A, Monnet F, Gigou M, Humbert L, Rainteau D, Azoulay D, Castaing D, Gillon MC, Samuel D, Duclos-Vallée JC, Tordjmann T. Immediate neuroendocrine signaling after partial hepatectomy through acute portal hyperpressure and cholestasis. J Hepatol. 2011;54:481–488. doi: https://doi.org/10.1016/j.jhep.2010.07.012.

130. Matsuo K, Hiroshima Y, Yamazaki K, Kasahara K, Kikuchi Y, Kawaguchi D, Murakami T, Ishida Y, Tanaka K. Immaturity of Bile Canalicular–Ductule Networks in the Future Liver Remnant While Associating Liver Partition and Portal Vein Occlusion for Staged Hepatectomy (ALPPS). Ann Surg Oncol. 2017;24:2456–2464. doi: 10.1245/s10434-017-5922-3.

131. de Haan LR, Verheij J, van Golen RF, Horneffer-van der Sluis V, Lewis MR, Beuers UHW, van Gulik TM, Olde Damink SWM, Schaap FG, Heger M, Olthof PB. Unaltered Liver Regeneration in Post-Cholestatic Rats Treated with the FXR Agonist Obeticholic Acid. Biomolecules. 2021;11. doi: 10.3390/biom11020260. Cited: in: : PMID: 33578971.

132. de Graaf W, Heger M, Spruijt O, Maas A, de Bruin K, Hoekstra R, Bennink RJ, van Gulik TM. Quantitative assessment of liver function after ischemia-reperfusion injury and partial hepatectomy in rats. J Surg Res. 2012;172:85–94. doi: 10.1016/j.jss.2010.06.038. Cited: in: : PMID: 20869070.

133. de Graaf W, Bennink RJ, Heger M, Maas A, de Bruin K, van Gulik TM. Quantitative assessment of hepatic function during liver regeneration in

a standardized rat model. J Nucl Med. 2011;52:294–302. doi: 10.2967/jnumed.110.078360. Cited: in: : PMID: 21233172.

134. Xiong H, Yoshinari K, Brouwer KLR, Negishi M. Role of constitutive androstane receptor in the in vivo induction of Mrp3 and CYP2B1/2 by phenobarbital. Drug Metab Dispos. 2002;30:918–923. doi: 10.1124/dmd.30.8.918. Cited: in: : PMID: 12124310.
135. Wagner M, Fickert P, Zollner G, Fuchsbichler A, Silbert D, Tsybrovskyy O, Zatloukal K, Guo GL, Schuetz JD, Gonzalez FJ, Marschall HU, Denk H, Trauner M. Role of farnesoid X receptor in determining hepatic ABC transporter expression and liver injury in bile duct-ligated mice. Gastroenterology. 2003;125:825–838. doi: 10.1016/s0016-5085(03)01068-0. Cited: in: : PMID: 12949728.
136. Padrissa-Altés S, Bachofner M, Bogorad RL, Pohlmeier L, Rossolini T, Böhm F, Liebisch G, Hellerbrand C, Koteliansky V, Speicher T, Werner S. Control of hepatocyte proliferation and survival by Fgf receptors is essential for liver regeneration in mice. Gut. 2015;64:1444–1453. doi: 10.1136/gutjnl-2014-307874. Cited: in: : PMID: 25416068.
137. Otsuka N, Yoshioka M, Abe Y, Nakagawa Y, Uchinami H, Yamamoto Y. Reg3α and Reg3β Expressions Followed by JAK2/STAT3 Activation Play a Pivotal Role in the Acceleration of Liver Hypertrophy in a Rat ALPPS Model. Int J Mol Sci. 2020;21. doi: 10.3390/ijms21114077. Cited: in: : PMID: 32517345.
138. Shi H, Yang G, Zheng T, Wang J, Li L, Liang Y, Xie C, Yin D, Sun B, Sun J, Wang H, Pan S, Jiang H, Lau W, Liu L. A preliminary study of ALPPS procedure in a rat model. Sci Rep. 2015;5:17567. doi: 10.1038/srep17567. Cited: in: : PMID: 26631552.
139. Friedman JR, Nunnari J. Mitochondrial form and function. Nature. 2014;505:335–343. doi: 10.1038/nature12985. Cited: in: : PMID: 24429632.
140. Azzolin L, Basso E, Argenton F, Bernardi P. Mitochondrial Ca2+ transport and permeability transition in zebrafish (Danio rerio). Biochim Biophys Acta. 2010;1797:1775–1779. doi: 10.1016/j.bbabio.2010.07.002. Cited: in: : PMID: 20633532.

9. Bibliography of the candidate's publications

Σ IF: 27.005

9.1. Bibliography related to the thesis Σ IF: 15.007

1. M. H. Fard-Aghaie, A. Budai, **N. Daradics**, G. Horvath, K. J. Oldhafer, A. Szijarto, A. Fulop

The effects of physical prehabilitation: Improved liver regeneration and mitochondrial function after ALPPS operation in a rodent model.

Journal of Hepato-Biliary-Pancreatic Sciences 28(8):692-702 (2021)

IF: 3.149

2. N. Daradics*, P. B. Olthof*, A. Budai, M. Heger, T. M. van Gulik, A. Fulop, A. Szijarto

The Role of Farnesoid X Receptor in Accelerated Liver Regeneration in Rats Subjected to ALPPS

Current Oncology 28(6):5240-5254 (2021)

IF: 3.109

3. N. Daradics, G. Horvath, L. Tretter, A. Paal, A. Fulop, A. Budai, A. Szijarto

The effect of Cyclophilin D depletion on liver regeneration following associating liver partition and portal vein ligation for staged hepatectomy

PLoS One 17(7):e0271606 (2022)

IF: 3.752

4. N. Daradics, K. Levay, I. Horvath, N. Kovacs, D. Mathe, K. Szigeti, A. Szijarto, A. Fulop

Physical prehabilitation improves the postoperative outcome of associating liver partition and portal vein ligation for staged hepatectomy in experimental model

Scientific Reports 12, Article number: 19441 (2022)

IF: 4.997

9.2. Bibliography not related to the thesis Σ IF: 11.998

5. K. Lévay*, N. Daradics*, T. Horváth, T. Kovács, A. Fülöp, A. Szijártó
Case report of actinomycotic liver abscess following COVID-19 infection
Annals of Medicine and Surgery 82 Paper: 104525, 4 p. (2022)
IF: -

6. B. Ágg, B. Szilveszter, **N. Daradics**, K. Benke, R. Stengl, M. Kolossváry, M. Pólos, T. Radovits, P. Ferdinandy, B. Merkely, P. Maurovich-Horvat, Z. Szabolcs
Increased visceral arterial tortuosity in Marfan syndrome.
Orphanet Journal of Rare Diseases 15;15(1):91. (2020)
IF: 4.123

7. R. Stengl, B. Ágg, B. Szilveszter, K. Benke, **N. Daradics**, B. Ruskó, B. Vattay, B. Merkely, M. Pólos, Z. Szabolcs
Case Report: Morphological Characterization and Long-Term Observation of Bilateral Sequential Internal Mammary Artery Aneurysms in a Patient With Confirmed FBN1 Mutation.
Frontiers in Cardiovascular Medicine 16;8:697591. (2021)
IF: 5.848

8. K. Benke, B. Ágg, J. Meienberg, AM. Kopps, N. Fattorini, R. Stengl, **N. Daradics**, M. Pólos, A. Bors, T. Radovits, B. Merkely, J. De Backer, Z. Szabolcs, G. Mátyás
Hungarian Marfan family with large *FBN1* deletion calls attention to copy number variation detection in the current NGS era.
Journal of Thoracic Disease 10(4):2456-2460. (2018)
IF: 2.027

DOI:10.14753/SE.2023.2809

10. Acknowledgements

I would like to express my sincere gratitude to my supervisor and chair of the Department of Surgery, Transplantation and Gastroenterology, *Professor Attila Szijártó*, for his guidance and support during the course of my PhD. His immense knowledge and plentiful experience have encouraged me all the time in my academic research.

I am also extremely grateful to the head of the Experimental Surgical Research Center, *Dr. András Fülöp*, without whom this endeavor would not have been possible. His treasured support shaped not only my experiment, but also my scientific knowledge and perspective. My gratitude extends to *Dr. Klára Lévay* and the members of the Experimental Surgical Research Center, for their kind help and support in my work.

I am also thankful for the national and international collaboration partners:
Dr. Gábor Lotz and *Dr. András Budai* from the Department of Pathology, Forensic and Insurance Medicine; *Prof. László Tretter* and *Dr. Gergő Horváth* from the Department of Medical Biochemistry; *Dr. Krisztián Szigeti*, *Dr. Máthé Domokos* and *Ildikó Horváth* from the Department of Biophysics and Radiation Biology; *Prof. Karl J. Oldhafer* and *Dr. Mohammad Fard-Aghaie* from Asklepios Campus, Hamburg; *Prof. Thomas M. van Gulik*, *Michal Heger* and *Pim Olthof* from Academic Medical Center, Amsterdam.

Finally, my deepest gratitude goes to my beloved ones. I am forever indebted to my parents for giving me love, opportunities and experiences that have shaped me who I am. My friends, who made me laugh even in my darkest hours, keeping my spirits to go on the road. And my fiancée, for always seeing the best version of me, making me become it.